



*FACULTAD
DE
CIENCIAS*

One dimensional model in crowd dynamics including pushing forces

(Modelo unidimensional de dinámica de multitudes incluyendo fuerzas de empuje)

Trabajo de fin de Grado
para acceder al

GRADO EN MATEMÁTICAS

Autor: Juan Claramunt González

Director: Luis Alberto Fernández

Mayo 2016

This research has been conducted mainly at the Institute for Computational and Experimental Research in Mathematics (ICERM) at Brown University, RI, USA from June 2015 to August 2015. It has been carried out with the collaboration of Jeremy Ariche, student of Morehouse College (Atlanta, Georgia) and Timothy Valicenti, student of Brown University (Providence, Rhode Island) and the support of Stefan Klajbor and Vadim Zharnitsky, PhD student and professor respectively at University of Illinois at Urbana-Champaign (Urbana-Champaign, Illinois).

Contents

1	Abstract	4
2	Introduction	4
3	General Description of the model	6
4	Forces	8
4.1	Overview	8
4.2	Normal Force	8
4.3	Pushing Forces	10
4.3.1	Heaviside Force	10
4.3.2	Anti-Plastic Force	11
4.3.3	Plastic force	12
5	The Model in equations	13
6	Measuring the results	15
6.1	Physical Quantities	15
6.1.1	Energy	15
6.1.2	Density	17
7	Simulations	18
7.1	Setup	18
7.1.1	Initial configurations	18
7.1.2	Mass distribution	21
7.1.3	Length of the Interval and Slack	22
7.2	Results	22
7.2.1	Simulations with 2 pedestrians	23
7.2.2	Simulations with 50 pedestrians	31
7.2.3	Simulations with more than 50 pedestrians	45
7.3	Other observations	46
8	Conclusions	48
9	Limitations of the model	49
10	Benefits of the model	50
11	References	51
12	Appendix	52
12.1	Dormand-Prince method	52
12.2	A preliminary study about existence and uniqueness of solution of our ODE's system with discontinuous terms	53
13	Appendixes references	61

Agradecimientos

En primer lugar me gustaría agradecer tanto a la Universidad de Cantabria como a la Universidad de Brown a través del ICERM la oportunidad de hacer este trabajo con la colaboración de otros grandes estudiantes y profesores.

Me gustaría agradecer también a mi familia por su apoyo, por darme la libertad de hacer las cosas que he querido y como he querido.

También agradecer a Guadalupe su apoyo, su ayuda y su constante lucha contra mi inmovilismo. Sin ella este proyecto no se hubiese llevado a cabo ni yo sería quien soy hoy.

Asimismo, agradecerles a mis amigos los buenos ratos juntos, porque no todo en esta vida es estudiar y trabajar.

No me puedo olvidar tampoco de las otras dos personas más importantes en este proyecto como son Tim Valicenti y Jeremy Ariche con los que compartí tanto los buenos como los malos momentos en el desarrollo de esta idea.

También he de agradecer a tres personas de gran importancia en este trabajo como son Luis Alberto Fernández, Stefan Klijbor y Vadim Zharnitsky. Ellos han sido la voz de la experiencia que ha guiado a este joven barco a buen puerto.

Por último me gustaría agradecer a todas aquellas personas que me han permitido llegar hasta aquí, a quienes han confiado en mi y a quienes me han ayudado a ser quien soy.

1 Abstract

Se formula un modelo matemático de dinámica de multitudes mediante un sistema de EDO no lineales y con términos discontinuos en el cual se han introducido las fuerzas de empuje como posible factor causante de los accidentes y situaciones potencialmente mortíferas. Asimismo, se han definido términos como la energía o la densidad aplicados a este modelo para poder medir los resultados obtenidos. Se presentan simulaciones para diversas configuraciones iniciales y diferentes masas correspondientes a las personas que conforman la multitud. Se han obtenido resultados que si bien no permiten predecir para cualquier situación dónde estarán los puntos de peligro, si que permiten a corto plazo y con una configuración inicial dada determinar en qué puntos podrían producirse accidentes. Finalmente, se ha podido concluir que la introducción de fuerzas de empuje que aumentan la energía, también aumenta los puntos con mayor densidad máxima en el sistema y por tanto las posibilidades de que ocurran desgracias.

Palabras clave: multitud, dinámica, ecuaciones diferenciales ordinarias (EDO), modelo matemático, sistema de ecuaciones.

A model in crowd dynamics has been formulated in which we have introduced pushing forces as a factor that increases the risk in crowds. In order to measure this risk, important physical quantities have been defined such as the energy or the density specifically for this model. Moreover, we have considered different initial configurations and several mass configurations in order to test the model under different conditions. The obtained results show an unpredictable behavior for initial conditions; however, we can detect high density peaks, and consequently risky areas, in the studied initial configurations and always in the short-term. Furthermore, we find that pushing forces that increase energy also increase the areas where density is over dangerous levels.

Key words: crowd, dynamics, ordinary differential equations (ODE), mathematical model, system of equations.

2 Introduction

Lately, there has been growing concerns regarding the proliferation of people across the world. Specifically, under high densities, dangers of stampeding effects in densely populated areas have been observed. In the last 25 years hundreds of people have died because of stampedes in crowds. Cities as New York (87 deaths in 1990), Los Angeles (51 deaths in 1992), Mandi Dabwali in India (441 deaths in 1995), Inchon in South Korea (54 death in 1999), Tokio (44 deaths in 2001), Ho Chi Minh city (61 deaths in 2001), Rhode Island (over 100 deaths in 2003), Bombay (51 deaths in 2004), Manila (79 deaths in 2006), Duisberg (Loveparedede stampede in 2010 killed 21 people) and especially Mecca where on 24 September 2015 about 700 pilgrims were killed in a stampede and over 3,200 have died in the last 25 years, have known what crowds are able to cause [3]. There are many other examples of deaths caused by stampedes, so the development of models to predict crowd dynamics could allow

us to save many lives. Furthermore, knowledge in this field will aid businesses in designing optimally structured facilities for panic situations at minimal cost.

Much research has been conducted in an effort to understand these phenomena, but much remains to understand. Current research suggests that crowds behave much like a fluid. However, this model fails to be sufficient for all population scenarios. Thus, we seek an appropriate model that accurately simulates the dynamics of a panicking crowd and normal crowd activity.

How are models in crowd dynamics nowadays? Essentially, two distinct rudimentary approaches are utilized to model crowd behavior. The first approach involves treating pedestrians as distinct individuals and selecting appropriate algorithms to simulate walking behavior. This method tends to give more reliable results when pedestrian count is low as in [4]. When large crowds develop, it becomes reasonable to treat the entire crowd as a whole and model them using a gas-kinetic or fluid dynamic framework [5] [7]. Each model has its own advantages and disadvantages. The discrete model can be favorable in terms of flexibility. For instance, one can consider behavioral forces acting on a system, influencing the trajectories of pedestrians. In more recent developments, D. Helbing has made significant progress in the field of crowd dynamics. While abandoning most prior assumptions of crowd behavior dynamics, he used heuristic observations from films to adopt a flexible microscopic description of crowd behavior. Helbing's models are able to predict many social phenomena including dangerous pressure build-ups, clogging effects at bottlenecks, and ignorance of nearby exits due to herding [1][2].

We are particularly interested in a specific physical event that occurs in crowd dynamics. We aim to model the effects of pushing for dense crowd situations for the simplified scenario of a one dimensional line. We would like to explore physical phenomena that arise as a result of the pushing force.

The model which will be presented in this paper is not enough realistic yet to provide predictions for any scenario, but it is enough to provide a potential cause for the stampedes or other risky situations related with crowds: a pushing force.

Upon modeling crowd behavior in one-dimensional space with each respective pushing force, we seek to measure the system's total energy and pressure. The goal of our model is to find high densities peaks in crowd dynamics. Find these potentially dangerous areas could help to reduce the number of deaths caused by crowds.

The results of this model allows us to find a relation between energy, pushing forces and high density peaks, so that different pushing forces lead to either dangerous behavior whenever they increase the energy or stable situations if they decrease the energy. As a consequence of this fact, we can conclude thanks to this simple model that pushing forces could be one of the factors that cause dangerous situations such as stampedes and overcrowded areas.

3 General Description of the model

We will consider a one-dimensional finite interval of length L where the boundaries are the walls of a thin hallway (see Fig. 1).

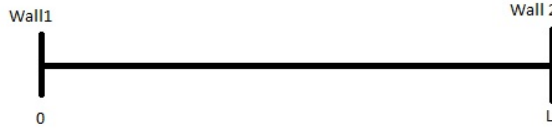


Figure 1: Interval and walls

Pedestrians are populated within the given region. We will choose to represent each pedestrian as an interval centered at the point x_i , as the position of the mass center of the person i , x_i , depends on time we will denote it as $x_i(t)$, with a fixed radius r that represents a pedestrian shoulder width (see Fig. 2).

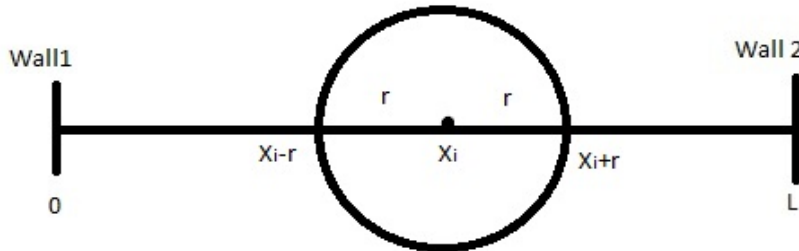


Figure 2: Interval, walls and a pedestrian

Hence, each pedestrian will occupy a region of length $2r$, the interval $(x_i(t) - r, x_i(t) + r)$. We will require that for all time t , $x_i(t) \in (0, L)$ and $x_i(t) < x_{i+1}(t)$. This condition is reasonable as this is a one-dimensional model (in higher dimensions this condition would turn to $x_i(t) \neq x_j(t)$ if $i \neq j$ while in our one-dimensional model, as people cannot switch positions by moving in other directions, it is enough with $x_i(t) < x_{i+1}(t)$). Physically, this means that no pedestrian's center of mass is allowed to cross one another or a wall.

An example of the distribution of the pedestrians along the interval can be observed in figure 3

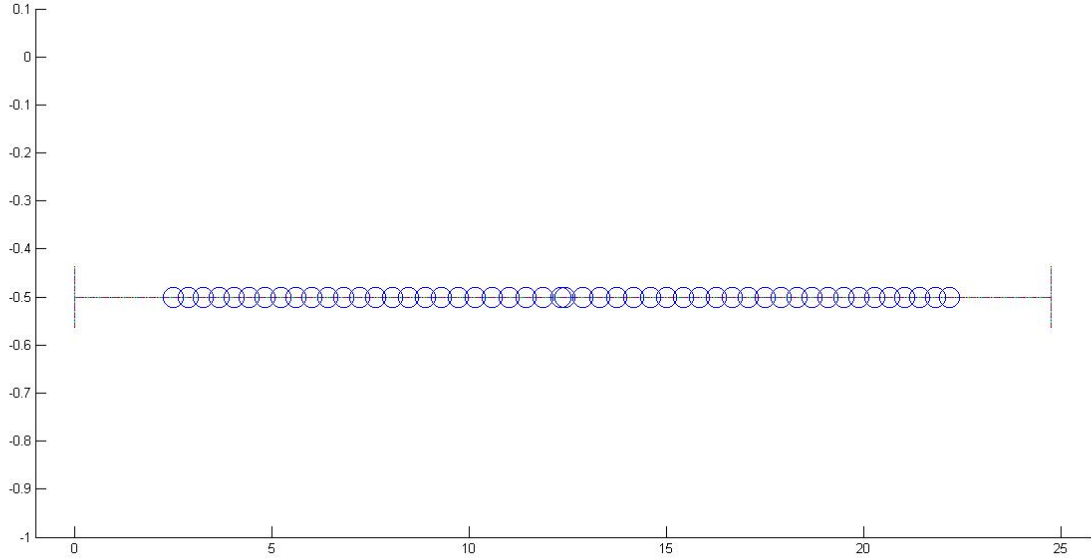


Figure 3: Initial configuration with 50 pedestrians

We are particularly interested in the qualitative behavior of the pedestrians due to the physical interactions between them. To capture this notion we define physical contact as an overlap between two pedestrian's intervals. We define the overlap $\Delta_i(t)$ between pedestrian i and $i+1$ as:

$$\Delta_i(t) := (x_i(t) + r) - (x_{i+1}(t) - r) = x_i(t) - x_{i+1}(t) + 2r \quad (1)$$

Careful consideration must be taken into account when a pedestrian interacts with the boundary. Thus, we define the overlap between pedestrian $x_1(t)$ and the left boundary wall as:

$$\Delta_L(t) := -x_1(t) + r \quad (2)$$

Similarly, we define the overlap between pedestrian $x_n(t)$ and the right boundary as the following:

$$\Delta_R(t) := x_n(t) + r - L \quad (3)$$

Since we restrict to the case $x_i(t) \in (0, L)$ and $x_i(t) < x_{i+1}(t)$ for all time t , we obtain that $\Delta_L(t), \Delta_R(t) \in (r - L, r)$ and $\Delta_i(t) \in (2r - L, 2r)$

We can understand this definitions better through the following figure. (4)

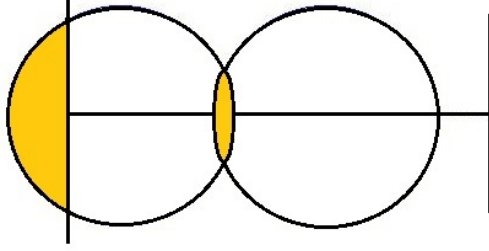


Figure 4: Example of the overlaps between pedestrians and pedestrian one and the wall

Along the paper and in order to emphasize the dependence of Δ on the position we will refer to $\Delta_R(t)$, $\Delta_L(t)$ and $\Delta_i(t)$ as Δ_R , Δ_L and Δ_i respectively.

4 Forces

4.1 Overview

One of the main parts of developing a crowd dynamics model is to find some functions which can describe the behavior of the forces that can be found in a crowd.

For our model, we will consider only the physical forces that influence the trajectories of the pedestrians. We assume that a normal force is necessary to prevent people from crossing paths or the walls. We also consider different candidates for a pushing force, which is the most important one in this model because, as we said previously, we are looking for high density peaks induced by pushing forces.

4.2 Normal Force

When two humans are in contact, physical considerations imply the existence of a normal force between them. This force is responsible for preventing pedestrians from crossing each other, one of the given conditions of this model. Provided that two pedestrians are in physical contact, we define the normal force, F^N , as follows:

$$F^N(\Delta_i(t)) := \begin{cases} \kappa \tan\left(\frac{\pi}{2} \frac{\Delta_i(t)}{2r}\right) & \text{if } \Delta_i(t) > 0 \\ 0 & \text{if } \Delta_i(t) \leq 0 \end{cases} = \kappa \tan\left(\frac{\pi}{2} \frac{\max(\Delta_i(t), 0)}{2r}\right) \quad (4)$$

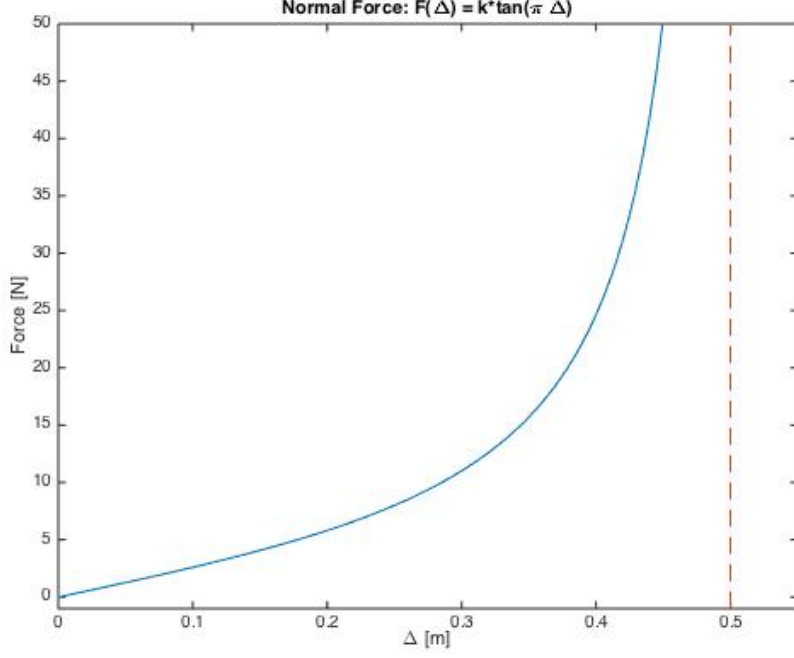


Figure 5: Tangent graph

where κ is a proportionality constant corresponding to the intensity of the force. Definition (4) must be slightly altered to handle the pedestrians who are able to come in contact with the wall.

$$F^{NL}(t) := \begin{cases} \kappa \tan\left(\frac{\pi}{2} \frac{\Delta_L(t)}{r}\right) & \text{if } \Delta_L(t) > 0 \\ 0 & \text{if } \Delta_L(t) \leq 0 \end{cases} = \kappa \tan\left(\frac{\pi}{2} \frac{\max(\Delta_L(t), 0)}{r}\right) \quad (5)$$

$$F^{NR}(t) := \begin{cases} \kappa \tan\left(\frac{\pi}{2} \frac{\Delta_R(t)}{r}\right) & \text{if } \Delta_R(t) > 0 \\ 0 & \text{if } \Delta_R(t) \leq 0 \end{cases} = \kappa \tan\left(\frac{\pi}{2} \frac{\max(\Delta_R(t), 0)}{r}\right) \quad (6)$$

The work done by this force on a pedestrian is independent of the path a pedestrian traverses. The above choice of normal force is by no means a unique choice. In choosing this particular form we sought to capture the general qualitative behavior induced by a normal force, this is, the closer pedestrians are, the stronger normal force is.

This is the reason why we introduce a tangent function is to avoid pedestrians crossing each other, as there is a vertical asymptote at $\Delta = r$ if we consider the overlap between person 1 and the left wall or person n and the right wall or $\Delta = 2r$ otherwise.

4.3 Pushing Forces

It is natural to expect humans to begin to push each other in high density crowds. One of our goals is to model the effect of such a force on the trajectories of the pedestrians. As a consequence of this force, we expect to observe the high increase of density and wave-like behavior of the system under certain conditions. Thus, in modeling the pushing force we look for candidates that will cause the total energy to increase and will compare them without pushing forces and pushing forces which decreases energy. We propose several possible candidates for an appropriate pushing force F^P .

4.3.1 Heaviside Force

Our first approach is to model the pushing force as a constant force that is present whenever there is overlap. However, there should be a difference in the way it acts depending on whether the level of contact, what we call the overlap, is increasing or it is decreasing. In the case that the overlap is decreasing between two pedestrians (that is, $\dot{\Delta} \leq 0$ where $\dot{\Delta} = \frac{d\Delta}{dt}$) we expect a lag, $\Delta_0 > 0$, before pushing begins. That is, they need to be close enough for them to push. Then, we will assume that the push is a constant. When the overlap is increasing, we expect the pedestrians to push until they are comfortable. This results in a force of the form:

$$F^H(\Delta_i(t), \dot{\Delta}_i(t)) = \begin{cases} P & \text{if } \dot{\Delta}_i(t) > 0 \wedge \Delta_i(t) > 0 \\ 0 & \text{if } \dot{\Delta}_i(t) > 0 \wedge \Delta_i(t) \leq 0 \\ P & \text{if } \dot{\Delta}_i(t) \leq 0 \wedge \Delta_i(t) > \Delta_0 \\ 0 & \text{if } \dot{\Delta}_i(t) \leq 0 \wedge \Delta_i(t) \leq \Delta_0 \end{cases} \quad (7)$$

$$= P \cdot H(\Delta_i(t)) \cdot H(\dot{\Delta}_i(t)) + P \cdot H(\Delta_i(t) - \Delta_0) \cdot H(-\dot{\Delta}_i(t)) \quad (8)$$

where $H(\Delta(t))$ is an alternative version of the Heaviside function:

$$H(x) = \begin{cases} 1 & \text{if } x > 0 \\ 0 & \text{if } x \leq 0 \end{cases} \quad (9)$$

In this case we take $H(0) = 0$ instead of $H(0) = 1$ or $H(0) = \frac{1}{2}$ as it is usual.

For convenience, we can also smooth this force and consider:

$$F^{HR}(\Delta_i(t), \dot{\Delta}_i(t)) := \begin{cases} \frac{P}{2} \left(\frac{2}{\pi} \arctan(\beta \Delta_i(t)) + 1 \right) & \text{if } \dot{\Delta}_i(t) > 0 \\ \frac{P}{2} \left(\frac{2}{\pi} \arctan(\beta(\Delta_i(t) - \Delta_0)) + 1 \right) & \text{if } \dot{\Delta}_i(t) \leq 0 \end{cases} \quad (10)$$

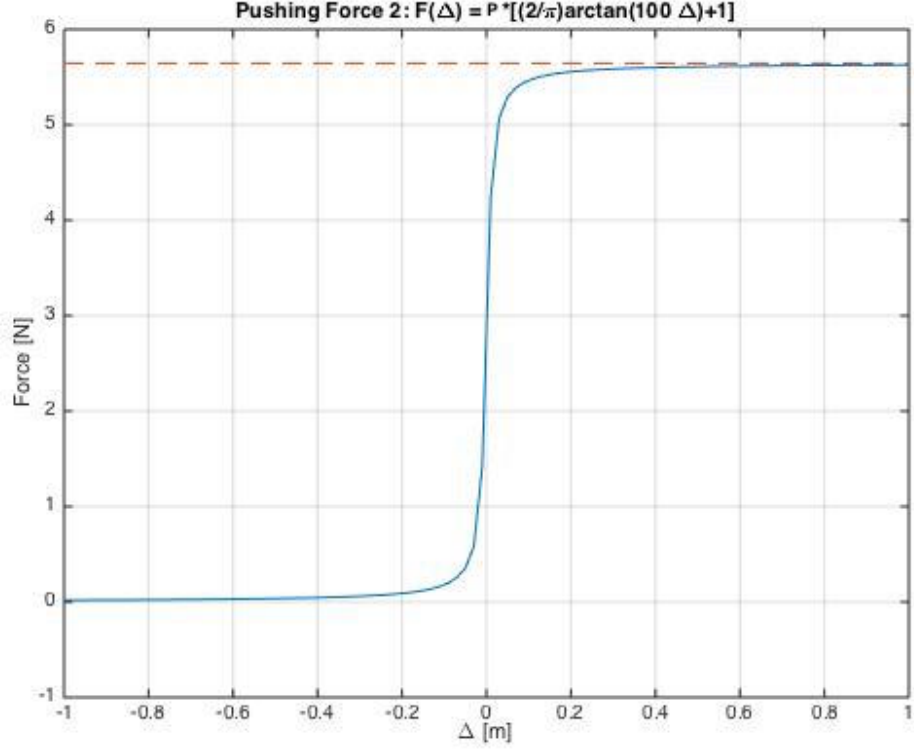


Figure 6: $f(x) = \arctan(x)$

where P is a constant that characterizes the intensity of the pushing force the pedestrian i feels from $i+1$. β is a large constant so that arctangent is essentially a step function. $\Delta_0 \geq 0$ is a threshold constant dictating when the pushing force should activate when the overlap is decreasing.

4.3.2 Anti-Plastic Force

It seems natural to consider that the intensity of the force depends on the level of overlap. When the overlap is increasing ($\dot{\Delta}_i \geq 0$), we model the pushing force as depending linearly on Δ_i with slope m passing through the origin (no push when $\Delta_i = 0$) up to $\Delta_i = 2r$ (maximum overlap). When the overlap is decreasing we also model it as depending linearly on Δ_i but with slope M , $0 < M < m$. This acts only when $\Delta_i \geq 0$ and for the purpose of computing, the equation would pass through the point $(d_0, 0)$ in the negative independent axis. Then, for the maximum overlap $2r$, we have the line equation $F^A(\Delta_i, \dot{\Delta}_i) - m \cdot 2r = M \cdot (\Delta_i - 2r)$. If we substitute and isolate, we obtain the value $d_0 = 2r - \frac{m \cdot 2r}{M} = 2r(1 - \frac{m}{M}) < 0$. This value satisfies that if $\Delta_i = 2r$ then $m\Delta_i = M(\Delta_i - d_0)$. This results in a force of the form

$$F^A(\Delta_i(t), \dot{\Delta}_i(t)) = \begin{cases} m\Delta_i(t) & \text{if } 0 \leq \dot{\Delta}_i(t) \wedge \Delta_i(t) > 0 \\ M(\Delta_i(t) - d_0) & \text{if } 0 > \dot{\Delta}_i(t) \wedge \Delta_i(t) > 0 \\ 0 & \text{if } \Delta_i(t) \leq 0 \end{cases} \quad (11)$$

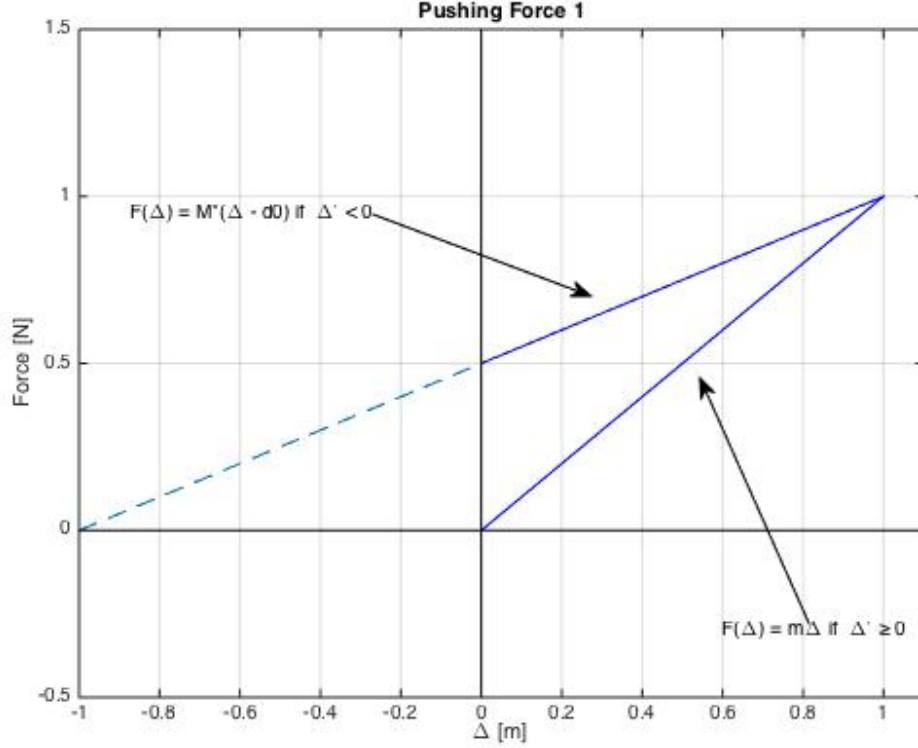


Figure 7: Anti-plastic force diagram

This can be better understood graphically by a single diagram reminiscent of stress-strain diagram in the theory of plasticity (see Fig. 7). Our force results in a "stress-strain" diagram with arrows opposite to these obtained in plasticity, hence why we use the moniker "anti-plastic" to describe it.

4.3.3 Plastic force

As one of our goals is to compare how our system works with different pushing forces we introduce a new one which we expect to decrease total energy. Again we consider that the intensity of the force depends on the level of overlap linearly. However in this case the slope is greater whenever $\dot{\Delta}_i \leq 0$, that is, when the overlap is decreasing. Then the pushing force depends linearly on Δ_i with slope m_p passing through the origin up to $\Delta_i = 2r$ if $\dot{\Delta}_i \geq 0$ as in the case of the anti-plastic pushing force. In case the overlap is decreasing the pushing force also depends linearly on Δ_i with slope M_p , $M_p > m_p > 0$. Then the definition of the plastic pushing force is

$$F^{Pl}(\Delta_i(t), \dot{\Delta}_i(t)) = \begin{cases} m_p \Delta_i(t) & \text{if } \dot{\Delta}_i(t) > 0 \wedge \Delta_i(t) > 0 \\ M_p(\Delta_i(t) - d_p) & \text{if } \dot{\Delta}_i(t) \leq 0 \wedge \Delta_i(t) > d_p \\ 0 & \text{otherwise} \end{cases} \quad (12)$$

where $d_p = 2r \cdot (1 - \frac{m_p}{M_p}) > 0$ is analogous to the point d_0 in the anti-plastic pushing force.

This force can be better understood observing the following diagram (see Fig. 8):

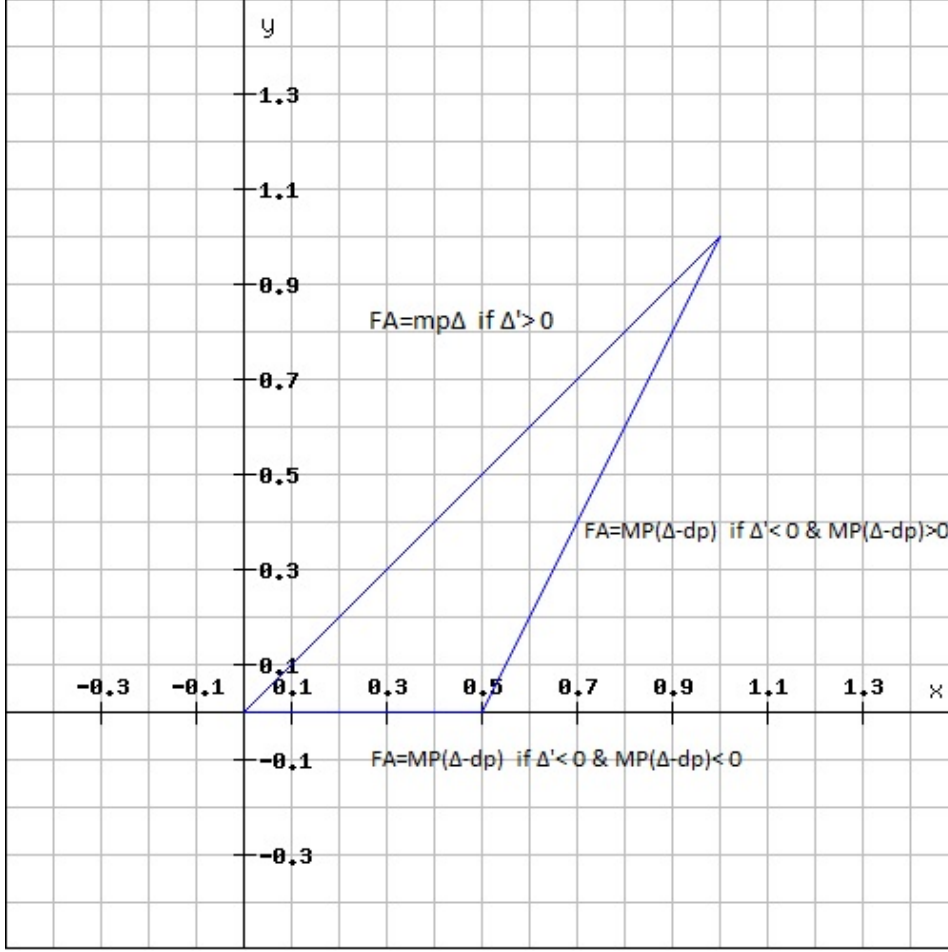


Figure 8: Plastic force diagram

5 The Model in equations

Given a choice of a pushing force F^P , which from now until the end will refer to any of the three pushing forces detailed before (this is P^{HR}, P^A and P^{Pl}), we consider the forces acting on each pedestrian i of our model. For example, person i , $i \in \{2, \dots, n-1\}$, is pushed by people $i-1$ and $i+1$ and in case of physical contact normal force between person i and person $i-1$ and normal force between person i and person $i+1$ come out. Then, we can then apply Newton's Second Law ($F = m\ddot{x}$) to obtain the following equation of motion:

$$\begin{aligned}
 m_i \ddot{x}_i(t) &= F^N(\Delta_{i-1}(t)) - F^N(\Delta_i(t)) + F^P(\Delta_{i-1}(t), \dot{\Delta}_{i-1}(t)) - F^P(\Delta_i(t), \dot{\Delta}_i(t)) \\
 &\quad \forall i \in \{2, \dots, n-1\}
 \end{aligned}
 \tag{13}$$

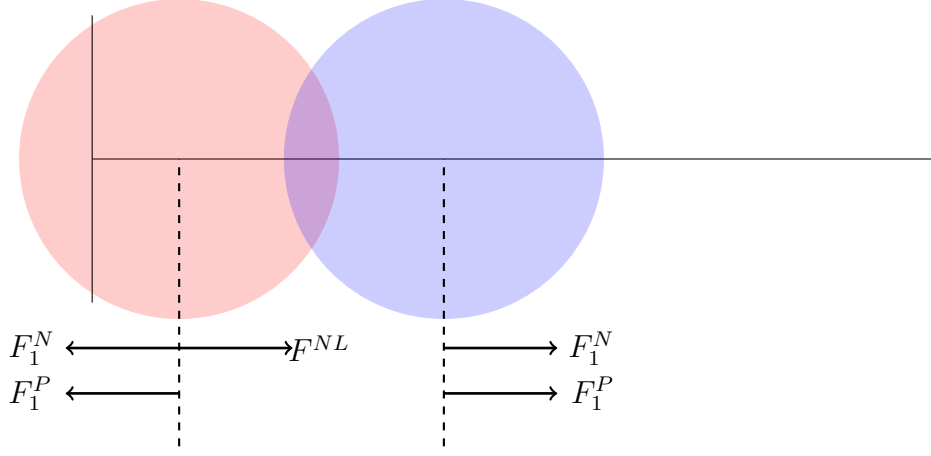


Figure 9: Representation of a two pedestrians system

Pedestrians near a wall do not feel a pushing force from the wall, and consequently we obtain the following equations:

$$m_1 \ddot{x}_1(t) = F^{NL}(t) - F^N(\Delta_1(t)) - F^P(\Delta_1(t), \dot{\Delta}_1(t)) \quad (14)$$

$$m_n \ddot{x}_n(t) = -F^{NR}(t) + F^N(\Delta_{n-1}(t)) + F^P(\Delta_{n-1}(t), \dot{\Delta}_{n-1}(t)) \quad (15)$$

As we observe in the diagram (9)

This results in a system of ordinary differential equations (ODE) of the form:

$$\left\{ \begin{array}{l} m_1 \ddot{x}_1(t) = F^{NL}(t) - F^N(\Delta_1(t)) - F^P(\Delta_1(t), \dot{\Delta}_1(t)) \\ m_2 \ddot{x}_2(t) = F^N(\Delta_1(t)) - F^N(\Delta_2(t)) + F^P(\Delta_1(t), \dot{\Delta}_1(t)) - F^P(\Delta_2(t), \dot{\Delta}_2(t)) \\ \vdots \\ m_i \ddot{x}_i(t) = F^N(\Delta_{i-1}(t)) - F^N(\Delta_i(t)) + F^P(\Delta_{i-1}(t), \dot{\Delta}_{i-1}(t)) - F^P(\Delta_i(t), \dot{\Delta}_i(t)) \\ \vdots \\ m_{n-1} \ddot{x}_{n-1}(t) = F^N(\Delta_{n-2}(t)) - F^N(\Delta_{n-1}(t)) + F^P(\Delta_{n-2}(t), \dot{\Delta}_{n-2}(t)) - F^P(\Delta_{n-1}(t), \dot{\Delta}_{n-1}(t)) \\ m_n \ddot{x}_n(t) = -F^{NR}(t) + F^N(\Delta_{n-1}(t)) + F^P(\Delta_{n-1}(t), \dot{\Delta}_{n-1}(t)) \end{array} \right. \quad (16)$$

We seek to understand the behavior of the solutions of this system numerically. In order to solve this system of ODE's we use the mathematical software MATLAB. In particular we have worked with the solver ODE45 (checking the results using other ode solvers such as ODE23) which is based on an explicit Runge-Kutta formula [8], the Dormand-Prince pair. For further information about the ode solver method see Appendix 1.

Another important point to understand is the existence and uniqueness of solution for the system of equations (16). After an initial analysis we find that this problem requires more effort than what was initially expected and it is studied in Appendix 2.

In the next section, we consider those qualities of physics related to this system which are of interest for the modeling purposes.

6 Measuring the results

We need to introduce several physical quantities to measure our results in order to check if the model works properly and to be able to compare the different results that we obtain from different simulations.

6.1 Physical Quantities

6.1.1 Energy

In choosing how to model the pushing force we sought to inject energy into the system by the inclusion of pushing. Thus, we derive here the expression for total energy.

The kinetic energy for our system is defined in the usual sense,

$$\sum_{i=1}^n KE_i = \sum_{i=1}^n \frac{1}{2} m_i v_i^2(t) = \sum_{i=1}^n \frac{1}{2} m_i \dot{x}_i^2(t) \quad (17)$$

where n is the number of people in the system.

There is also potential energy coming from the normal force (the pushing forces defined in this paper are not conservative). Recall that a force has potential if there exists a scalar function V such that:

$$NF = -\nabla V \quad (18)$$

where NF represents all normal forces and $\nabla = \sum_{i=1}^n \vec{e}_i \frac{\partial}{\partial x_i}$ being (x_1, \dots, x_n) the coordinates of our system and (e_1, \dots, e_n) the standard basis.

For the normal force, this is indeed the case and we can compute it by integrating along a solution of the system. So, let

$$NF = (F^{NL} - F^N(\Delta_1), F^N(\Delta_1) - F^N(\Delta_2), \dots, F^N(\Delta_{n-1}) - F^{NR}) \quad (19)$$

be the net normal force in the system and \vec{dr} the line element in \mathbb{R}^n . We can integrate over the solution $\vec{x} = (x_1(t), \dots, x_n(t))$ of the system to obtain:

$$V = - \int (-\nabla V) \cdot \vec{dr} = - \int (NF(t)) \cdot \vec{dr} \quad (20)$$

$$= \int F^{NL}(t) d\Delta_L + \int F^{NR}(t) d\Delta_R + \sum_{i=1}^{n-1} \int F^N(\Delta_i) d\Delta_i \quad (21)$$

By (21)

$$\begin{aligned}
V(x_1, \dots, x_n) = & -\frac{2\kappa r}{\pi} \log(|\cos(\frac{\pi}{2r} \max(\Delta_L, 0))|) - \frac{2\kappa r}{\pi} \log(|\cos(\frac{\pi}{2r} \max(\Delta_R, 0))|) - \\
& - \sum_{i=1}^{n-1} \frac{4\kappa r}{\pi} \log(|\cos(\frac{\pi}{4r} \max(\Delta_i, 0))|) + C_1
\end{aligned} \tag{22}$$

where C_1 is the integration constant and V is continuous (even for $\Delta_i = 0$). Previous equation (22) holds for $0 \leq \frac{\pi}{2r} \max\{\Delta_L, 0\} < \frac{\pi}{2}$, $0 \leq \frac{\pi}{2r} \max\{\Delta_R, 0\} < \frac{\pi}{2}$ and $0 \leq \frac{\pi}{4r} \max\{\Delta_i, 0\} < \frac{\pi}{2}$, $\forall i \in \{1, \dots, n-1\}$, for whenever $\Delta_L, \Delta_R < r$ and $\Delta_i < 2r$. This confirms that the normal force is conservative as expected and as we will see in the simulations.

Namely, if we consider the previous system of ordinary differential equations (16), then the total energy E of the system is given by,

$$E(t) = \frac{1}{2} \sum_{i=1}^n m_i \dot{x}_i^2(t) + V(x_1(t), \dots, x_n(t)) \tag{23}$$

as the pushing forces are not conservatives. With the addition of pushing forces, energy is expected to increase or decrease.

If we observe the energy evolve over time, we get the following equation,

$$\begin{aligned}
\frac{dE(t)}{dt} = & \sum_{i=1}^n m_i \dot{x}_i(t) \ddot{x}_i(t) + \dot{x}_1(t) \frac{\partial V}{\partial x_1}(x_1(t), \dots, x_n(t)) + \dots + \dot{x}_n(t) \frac{\partial V}{\partial x_n}(x_1(t), \dots, x_n(t)) = \\
= & \dot{x}_1(t) [m_1 \ddot{x}_1(t) + \frac{\partial V}{\partial x_1}(x_1(t), \dots, x_n(t))] + \dots + \dot{x}_n(t) [m_n \ddot{x}_n(t) + \frac{\partial V}{\partial x_n}(x_1(t), \dots, x_n(t))]
\end{aligned} \tag{24}$$

Since $NF = -\nabla V$,

$$\begin{aligned}
\frac{dE(t)}{dt} = & \dot{x}_1(t) [m_1 \ddot{x}_1(t) - F^{NL}(t) + F^N(\Delta_1(t))] + \dot{x}_2(t) [m_2 \ddot{x}_2(t) + \\
& + F^N(\Delta_2(t)) - F^N(\Delta_1(t))] + \dots + \dot{x}_{n-1}(t) [m_{n-1} \ddot{x}_{n-1}(t) + \\
& + F^N(\Delta_{n-1}(t)) - F^N(\Delta_{n-2}(t))] + \dot{x}_n(t) [m_n \ddot{x}_n(t) + F^{NR}(t) - F^N(\Delta(t))]
\end{aligned} \tag{25}$$

If we substitute $m_i \ddot{x}_i(t)$ by its value in equation (16) we obtain,

$$\begin{aligned}
\frac{dE(t)}{dt} = & \dot{x}_1(t) [-F^P(\Delta_1(t), \dot{\Delta}_1(t))] + \dot{x}_2(t) [F^P(\Delta_1(t), \dot{\Delta}_1(t)) - F^P(\Delta_2(t), \dot{\Delta}_2(t))] + \dots \\
& + \dot{x}_{n-1}(t) [F^P(\Delta_{n-2}(t), \dot{\Delta}_{n-2}(t)) - F^P(\Delta_{n-1}(t), \dot{\Delta}_{n-1}(t))] + \dot{x}_n(t) [F^P(\Delta_{n-1}(t), \dot{\Delta}_{n-1}(t))]
\end{aligned} \tag{26}$$

As $\Delta_i(t) = x_i(t) - x_{i+1}(t) + 2r$, then $\dot{\Delta}_i(t) = \dot{x}_i(t) - \dot{x}_{i+1}(t)$ and we finally obtain

$$\frac{dE(t)}{dt} = - \sum_{i=1}^{n-1} F^P(\Delta_i(t), \dot{\Delta}_i(t)) \frac{d\Delta_i}{dt} \quad (27)$$

Integrating over time, we get that the energy of the system that looks like,

$$E(t_2) - E(t_1) = \int_{t_1}^{t_2} dE = - \int_{t_1}^{t_2} \sum_{i=1}^{n-1} F^P(\Delta_i(t), \dot{\Delta}_i(t)) \dot{\Delta}_i dt \quad (28)$$

Finally it is important to notice that the energy is not measured in Joules as the mass is normalized (1 unit of mass is equal to 62 kg which is the average of human weight [6]). Then, we use J^* where $1J^* = 62J$.

6.1.2 Density

As said before, one our main goals is to find high density peaks induced by pushing forces. However, what does density mean in this system? There is no conventional definition of density in discrete crowd dynamics and consequently we need to define density in our system.

Our first idea to measure the density in a point $y \in [0, L]$ was to count the number of pedestrians who lies in the interval $(y - \delta, y + \delta) \subseteq [0, L]$ where $\delta > 0$ is a constant. Nevertheless, with that definition the distance of the pedestrians to the point y does not take into account and consequently we look for a different definition.

Consider an open interval J centered at $y \in [0, L]$. Let m be the usual Lebesgue measure on the line. We can define the density $\rho(J, t)$ at J at time t as the portion of individuals that lie in J at time t divided by the length of the interval.

This seems a natural option to measure "density" due to the fact that it provides a continuous measure of the amount of people in some locality of the interval $[0, L]$, and it will be mathematically expressed as,

$$\rho(J, t) := \frac{\sum_{i=1}^n m[J \cap (x_i(t) - r, x_i(t) + r)]}{m[J]} \quad (29)$$

Once the density for one point (this is, the density of one of its neighborhoods) has been defined, we are going to state how to measure density in the whole interval.

When studying the density in our system, we can partition the interval $[0, L]$ and measure the density at each partition j centered at y_j and in an interval J_j . One natural option is to study the case $y_j = O_j$ and $J_j = (O_j - \delta, O_j + \delta)$ for some fixed points O_j and a fixed non-negative constant δ . This provides the density to be,

$$\begin{aligned} \hat{\rho}_j(t) &:= \rho((O_j - \delta, O_j + \delta), t) = \\ &= \frac{\sum_{i=1}^n m[(O_j - \delta, O_j + \delta) \cap (x_i(t) - r, x_i(t) + r)]}{2\delta} \end{aligned} \quad (30)$$

If we take enough points O_j for a fixed δ we can cover the full interval $[0, L]$ and then obtain a measure of the density that covers each point $z \in [0, L]$. The smaller δ is and the more number of points O_j we study, the more accurate is this measure.

We expect the pushing force to have an effect on the local densities under certain conditions (initial configurations, etc.). This can be observed by studying the evolution of ρ_j all over the time.

It is important to remark that there is not units to measure the density in the way we do, so we are going to use what we called density units (d.u), where one unit is the density of only one person in the center of the interval we are measuring, always considering $\delta < r$.

7 Simulations

7.1 Setup

For the purpose of simulations, we consider four initial configurations. In all, we take initial velocities to be 0, this is $\dot{x}_i(0) = 0, \forall i \in \{L, R, 1 \dots, n\}$ as we believe simulations will be easier to analyze. Nevertheless, this assumption is critical (in some sense) from the point of view of proving existence and uniqueness of solution for the system (see Appendix 12.2).

It is of convenience to describe the initial configuration using the initial overlaps.

$$\Delta(0) = (\Delta_L(0), \Delta_1(0), \dots, \Delta_{n-2}(0), \Delta_{n-1}(0), \Delta_R(0)) \quad (31)$$

As r is prefixed, by definition of Δ_i we obtain the following system of equations,

$$\begin{cases} x_1(0) = r - \Delta_L(0) \\ x_2(0) = x_1(0) + 2r - \Delta_1(0) \\ \vdots \\ x_k(0) = x_{k-1}(0) + 2r - \Delta_{k-1}(0) \\ \vdots \\ x_{n-1}(0) = x_{n-2}(0) + 2r - \Delta_{n-2}(0) \\ x_n(0) = x_{n-1}(0) + 2r - \Delta_{n-1}(0) \end{cases} \quad (32)$$

that can be easily solved.

7.1.1 Initial configurations

Small Disturbance I

We want to observe what a small disturbance in the initial configuration might do to our system. First, we consider a configuration with slight overlap between any two pedestrians x_i and x_{i+1} , this is $\Delta_i > 0$, and zero everywhere else (here, "zero overlap" could mean also negative overlap, in fact, a situation where pedestrians are

not touching each other and consequently there is no overlap). That is, for the $\Delta(0)$ vector mentioned above, we require that for some i , $\Delta_i(0) = \eta$ where η is a positive constant. For the other positions $\forall j \neq i$, $\Delta_j(0) \leq 0$.

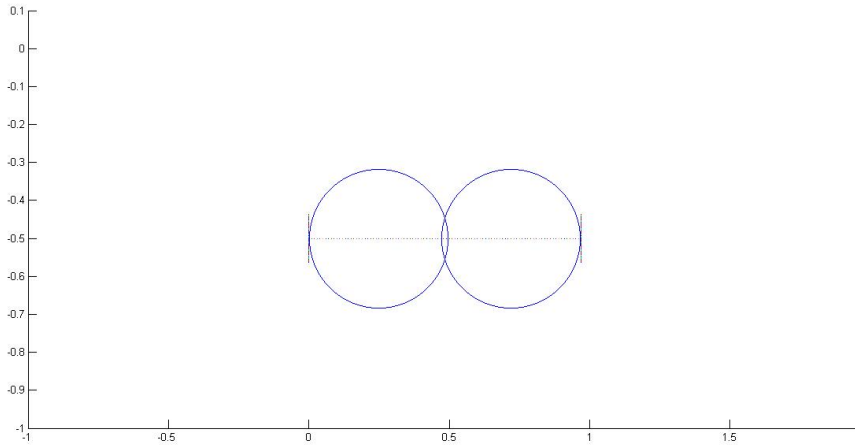


Figure 10: Small Disturbance I

Small Disturbance II

Another small disturbance we have considered is the one caused by a slight overlap between either person one and the left wall or person n and the right wall. This is, $\Delta_L(0) > 0$ and $\Delta_i(0) \leq 0$, $i \in \{1, \dots, n-1, R\}$ or $\Delta_R(0) > 0$ and $\Delta_i(0) \leq 0$, $i \in \{L, 1, \dots, n-1\}$.

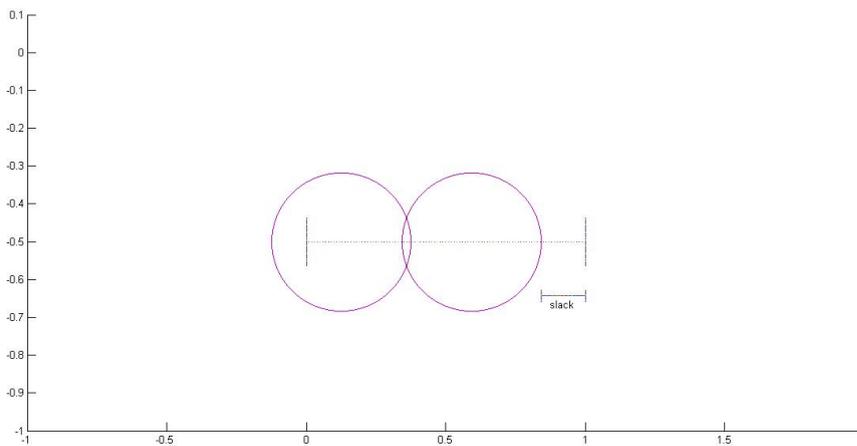


Figure 11: Small Disturbance II

Bell Curve Disturbance

Next, we consider a "bell curve" initial configuration in which overlap decreases between each pair of pedestrians as one progresses out toward the boundaries from the center.

Assuming that we have an even number of pedestrians, an odd number of spacing will correspond with the $\Delta(0)$. At $\Delta_{\frac{n}{2}}(0)$, it will have the maximal overlap. Then, as we increment to the left and right by one to $\Delta_{\frac{n}{2}-1}(0)$ and $\Delta_{\frac{n}{2}+1}(0)$ and after j steps $\Delta_{\frac{n}{2}-j-1}(0)$ and $\Delta_{\frac{n}{2}+j+1}(0)$, they will have a value that is equal or smaller than $\Delta_{\frac{n}{2}}(0)$ and than $\Delta_{\frac{n}{2}+i+1}(0)$, $\forall i \in \{0, \dots, j-1\}$ and $\Delta_{\frac{n}{2}-i-1}(0)$, $\forall i \in \{0, \dots, j-1\}$. This process is continued to the first and last delta.

If an odd number of pedestrians exist, then we must adjust our configuration slightly. In this case, $\Delta_{\frac{n-1}{2}}(0)$ and $\Delta_{\frac{n+1}{2}}(0)$ will both have the same maximal overlap. As we increment to the left and right in the same manner as mentioned above, the overlaps will have the same value and decrease.

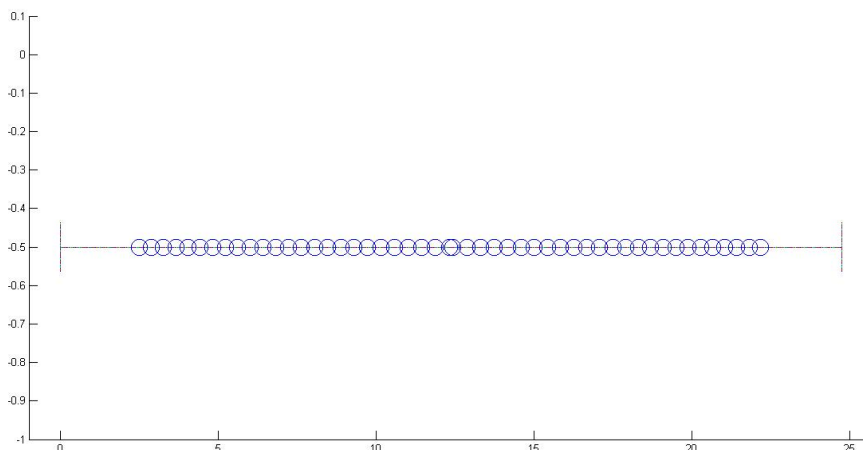


Figure 12: Bell curve disturbance

Alternating Disturbance

In the last initial configuration we consider the overlaps between every pair of pedestrian alternates in value: For $i = 2k, k \in \mathbb{N}$, $\Delta_i(0)$ receives the same non-negative value c_0 . For $i = 2k+1, k \in \mathbb{N}$, $\Delta_i(0)$ is assigned the non-negative value c_1 , $c_1 \neq c_0$.

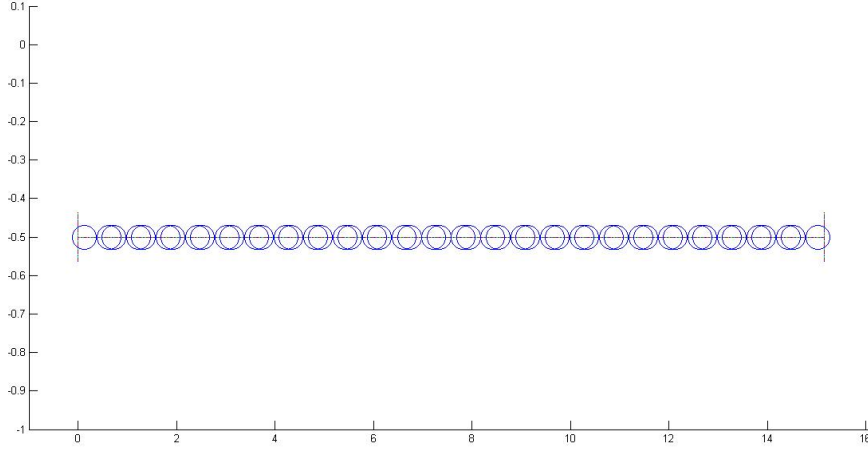


Figure 13: Alternating disturbance

7.1.2 Mass distribution

Due to the fact that masses are important variables in our system, we will use different mass distributions to find out how they affect to the results. Mass has been normalized in this model and consequently, 62 kilograms, the average human weight [6], are 1 unit.

Regular mass distribution

In this distribution everyone has the same mass. In general we will consider $m_i = 1, \forall i \in \{1, \dots, n\}$.

Massive center distribution

In this case, the person in the middle will have more mass than the others who have a mass of 1. As n could be even or odd we should define two cases.

If n is even, $m_{\frac{n}{2}} = 2$ and $m_i = 1, \forall i \in \{1, \dots, \frac{n}{2} - 1, \frac{n}{2} + 1, \dots, n\}$.

If n is odd, $m_{\frac{n+1}{2}} = 2$ and $m_i = 1, \forall i \in \{1, \dots, \frac{n+1}{2} - 1, \frac{n+1}{2} + 1, \dots, n\}$.

Less massive center distribution

In contrast of the massive center case, the person in the middle will have less mass than the others who also have a mass of 1. Similarly, as n could be even or odd we have to define two cases.

If n is even, $m_{\frac{n}{2}} = \frac{1}{2}$ and $m_i = 1, \forall i \in \{1, \dots, \frac{n}{2} - 1, \frac{n}{2} + 1, \dots, n\}$.

If n is odd, $m_{\frac{n+1}{2}} = \frac{1}{2}$ and $m_i = 1, \forall i \in \{1, \dots, \frac{n+1}{2} - 1, \frac{n+1}{2} + 1, \dots, n\}$.

Massive extremes configuration

In this distribution the extremes have more mass than the rest who remains with the average mass. Consequently, $m_1 = m_n = 2$ and $m_i = 1, \forall i \in \{2, \dots, n-1\}$.

Less massive extremes configuration

As previously, we consider the same case with less mass in the extremes. Then, the mass distribution is $m_1 = m_n = \frac{1}{2}$ and $m_i = 1, \forall i \in \{2, \dots, n-1\}$.

Random mass distribution

The last distribution randomize the mass configuration in order to know how random mass configurations diverge from regular mass distributions. We consider random numbers between $\frac{1}{2}$ and 2, then $m_i \in [\frac{1}{2}, 2], \forall i \in \{1, \dots, n\}$.

7.1.3 Length of the Interval and Slack

To this point, we have not said anything about the length of the interval. If we consider a system of n pedestrians and choose the interval to have length $L = 2rn$, observe that the initial configuration provided by having initial positions such that

$$\Delta_L(0) = 0, \Delta_R(0) = 0, \Delta_i(0) = 0, \quad i = 1, \dots, n-1$$

and initial velocities set to 0 induces a fixed point of the system. However, if we reduce the length of the interval by $\epsilon > 0$ ($L = 2nr - \epsilon$), it is impossible to keep initial positions so that

$$\Delta_i(0) = 0, \forall i \in \{L, 1, \dots, n-1, R\} \quad (33)$$

and then, we have perturbed the system away from the previous fixed point and generated movement due to the fact that now $\Delta_i > 0$ for at least one i such that $i \in \{L, 1, \dots, n-1, R\}$. It would be interesting to study the change (if any) in the dynamics, the energy, and the density as we vary and for different fixed choices of $\Delta(0)$.

We call the parameter ϵ the slack removed. Sometimes we will call no slack configuration when we remove ϵ from the system since when $\epsilon = 0$ the above mentioned fixed point is present. The interest in increasing ϵ comes from the desire to study what happens to an initial configuration as the room gets tighter.

Although we expect it to be less engaging, we will also consider to increase the length of the interval by $\epsilon > 0$.

7.2 Results

In this section results obtained through more than two hundred simulation under different conditions are exposed. The selection has been done in order to illustrate the most representative outcomes.

Before displaying the results related to simulations, it is convenient to define the values of the different common constants, shown in the table below. These values have been chosen by empirical facts and by trial and error mechanism. The magnitudes they represent have been introduced during the workflow of this report.

r	0.25
κ	8
β	100
P	0.28225
M	0.5
m	1
d_0	-0.25
M_p	2
m_p	1
d_p	0.25
ϵ^1	0.25

Once that the values of common constants have been set for every simulation we will describe each experiment.

Firstly, we start by the simulations in which the number of pedestrians, n is two (we do not take into consideration the case $n = 1$ for obvious reasons) in order to test whether the model works in the way it was developed. As it is the simplest scenario it is easier to understand the behavior of the model in different situations such as different mass configurations, initial conditions or forces. Then, some examples with more pedestrian are presented together with some interesting comments.

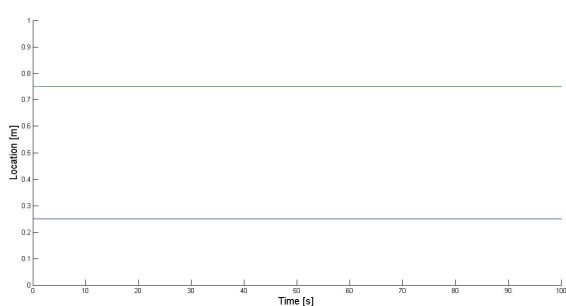
7.2.1 Simulations with 2 pedestrians

Simulation 1

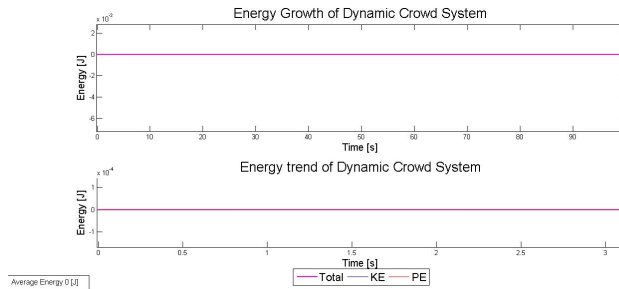
Initial configuration	No overlap
Slack	Yes
Mass configuration	Regular mass distribution
Pushing Force	Anti-plastic
Time [s]	100

In the first simulation we are willing to check that the model works properly in the case $\Delta_L \leq 0$, $\Delta_1 \leq 0$, $\Delta_R \leq 0$, this is, there is no initial overlap. We also introduce the four different graphs that are going to be shown in every simulation.

¹ ϵ takes this value only in cases of removed slack

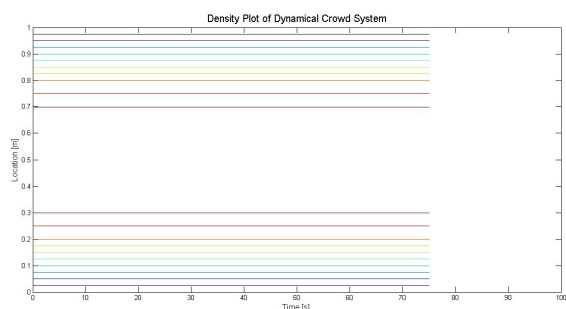


(a) Positions

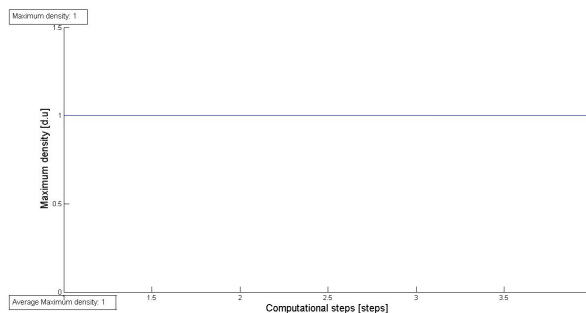


(b) Energy

Figure 14: Position and energy plots for simulation 1



(a) Density



(b) Maximum density

Figure 15: Density plots for simulation 1

In Fig. 14a (top-left) the position of each pedestrian along the interval in the y-axis and the time in the x-axis is observed. As we expected there is no position change by the given definition of the forces.

In Fig. 14b (top-right) the energy (y-axis) evolving with respect to the time is displayed. Here, the purple line represents total energy (the upper figure shows the total energy alone, while the lower shows all of them together), the blue line represents the potential energy and the red line represents the kinetic energy. We observe that all of them are constant as there is no position change and no overlap.

In the Fig. 15a (bottom-left) the density is presented where the y-axis shows the pedestrian's position and the x-axis shows time. In this plot the colors represent the density (each color line means a change in the density in a similar way to a contour line which can be found in a map). In this case there is no evolution over time in the density as a consequence of this initial configuration. Fig. 15b (bottom-right) shows how density evolves over computational steps (because we compute the density for each step). In this case it is obvious that density is constant and equal to 1, as there is no overlap and the interval in which we measure the density is $(x_i - r, x_i + r)$, $i \in \{1, 2\}$.

Simulation 2

Initial configuration	Small disturbance I
Slack	Yes
Mass configuration	Regular mass distribution
Pushing Force	None
Time	200

Due to checking purposes, we start by setting as the unique force the normal one because we want to review its behavior (meaning without pushing forces).

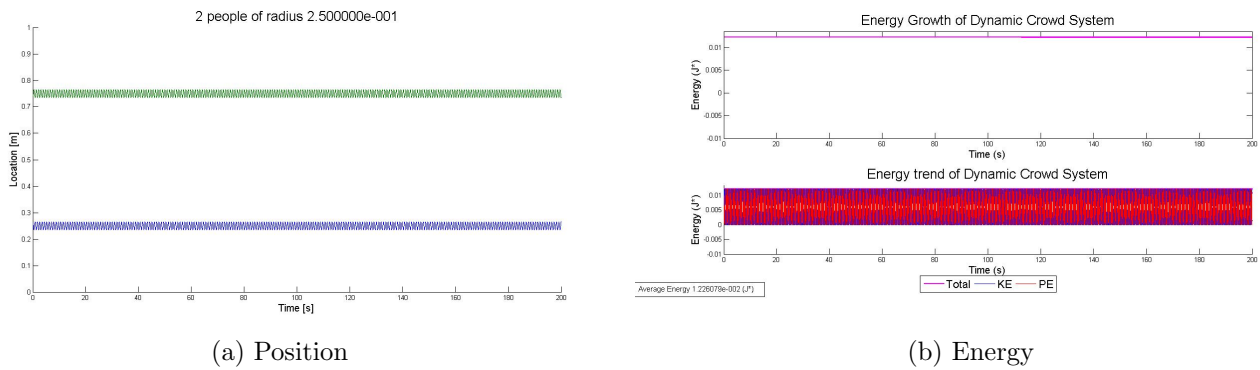


Figure 16: Position and energy plots for simulation 2

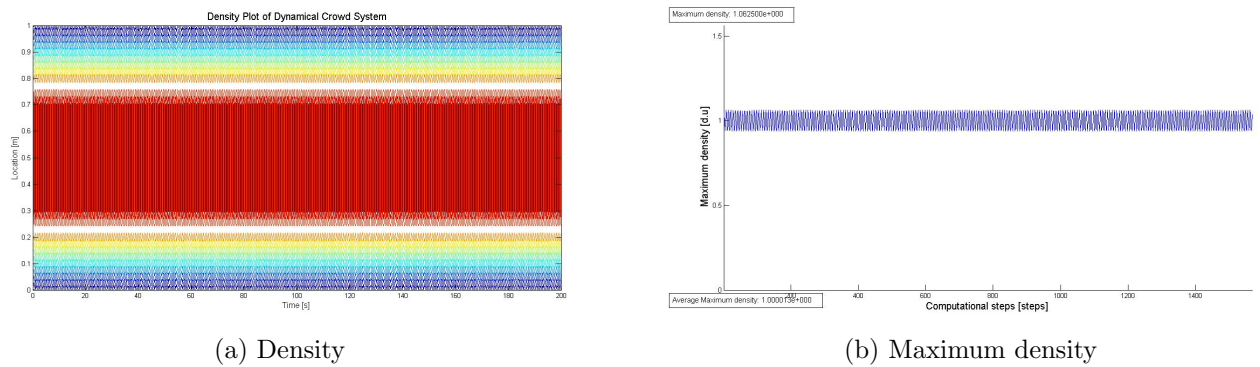


Figure 17: Density plots for simulation 2

We notice there is almost no movement, and the existing one is caused by the small disturbance (Fig. 16a). The amplitude of the oscillations is fixed, aspect which we can only find in simulations where the energy remains constant. Moreover, we find that there is no increment of the density over time in the long term and that density grows from the walls to the middle (Fig. 17a). Furthermore, we notice that the maximum density is also bounded (Fig. 17b).

The total energy is constant as the normal force is conservative (Fig. 16b). When the pedestrians are getting closer the potential energy grows while the kinetic energy

decreases and vice versa when they are separating.

Simulation 3

Initial configuration	Small disturbance I
Slack	No
Mass configuration	Regular mass distribution
Pushing Force	None
Time	200

The main goal of this simulation is to point out the difference between the existence of slack or not in the model.

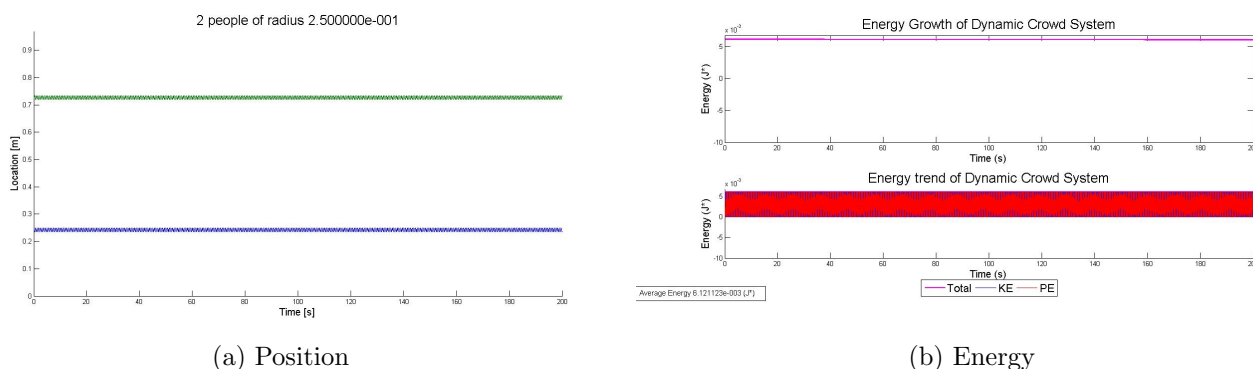


Figure 18: Position and energy plots for simulation 3

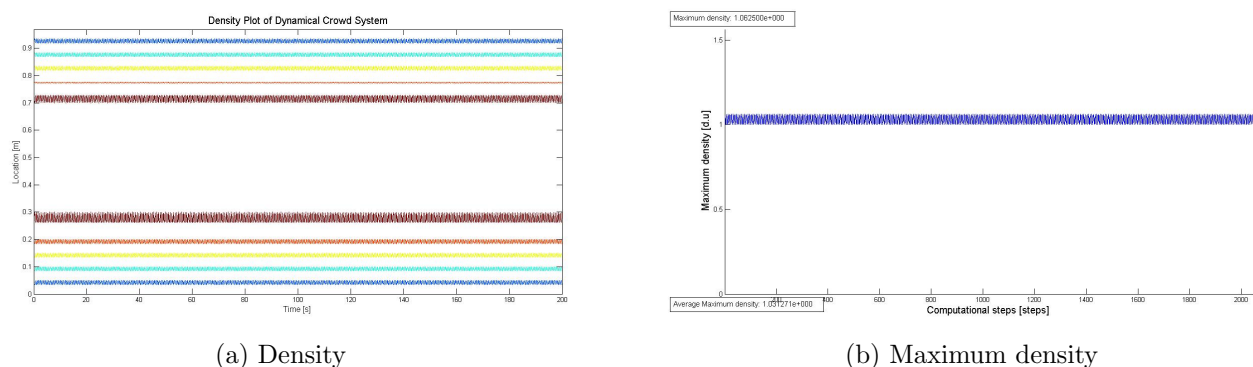


Figure 19: Density plots for simulation 3

The observed differences remark the fact that there is less amplitude in the oscillations and consequently less displacement with respect to the original positions (Fig. 18a). The total energy is about a half of the total energy shown at the second simulation (Fig. 18b) and there are less changes in density and in maximum density than the expected when there is less movement (Figs. 19a and 19b). As well as

previously, the energy is constant as a consequence of the conservation of energy in the case of the normal force.

Simulation 4

Initial configuration	Small disturbance I
Slack	Yes
Mass configuration	Regular mass distribution
Pushing Force	Anti-plastic
Time	200

In the fourth simulation a pushing force is introduced for the first time. In this case, the amplitude of the oscillations increase in contrast with the previous simulations without pushing force (Fig. 20a). This is a consequence of anti-plastic pushing force because, as we will see, other pushing forces does not increase this amplitude. It is also noticeable that energy rises as we expected when we designed the anti-plastic force (Fig. 20b). In the same way we detect that the density and the maximum density increase over time in the long term and mainly in the middle, between both pedestrians (Figs. 21a and 21b).

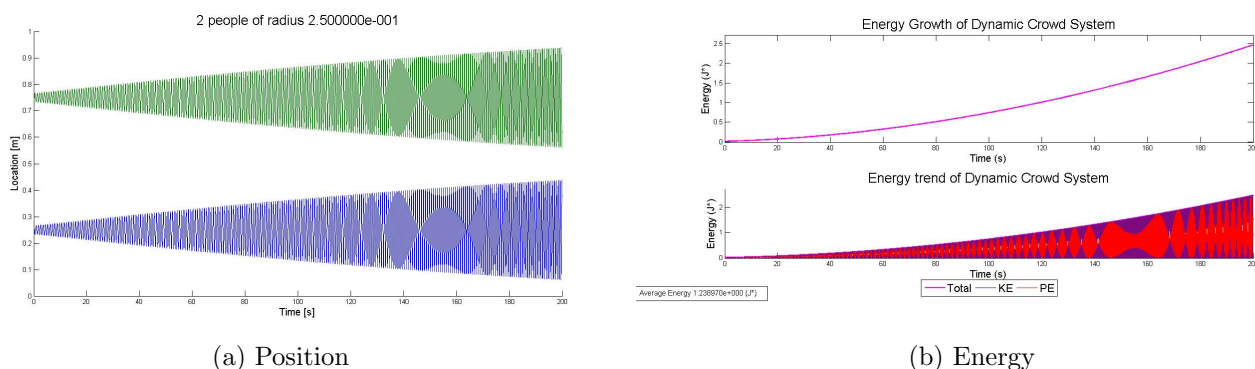


Figure 20: Position and energy plots for simulation 4

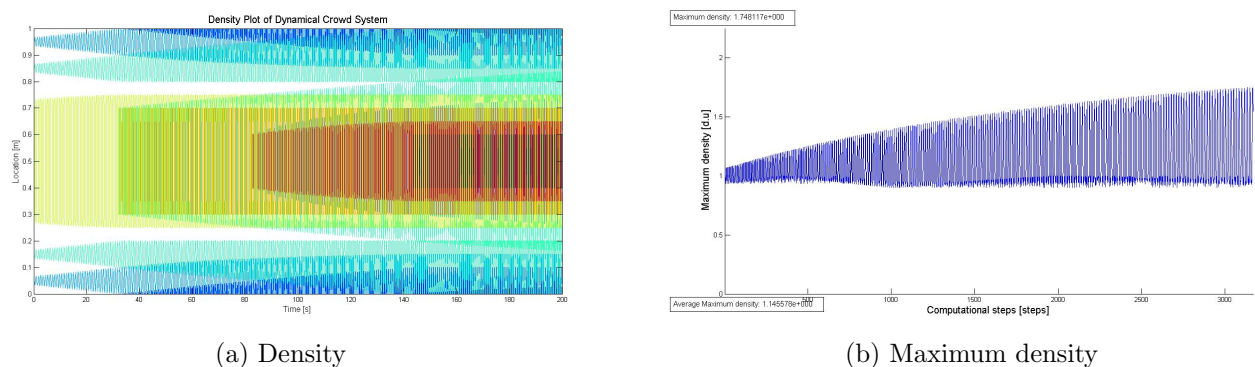


Figure 21: Density plots for simulation 4

Simulation 5

Initial configuration	Small disturbance I
Slack	No
Mass configuration	Regular mass distribution
Pushing Force	Anti-plastic
Time	200

In this simulation we corroborate that there is almost no difference between slack and no slack configurations. The tendencies are the same in positions (Fig. 22a), energy (Fig. 22b), density (Fig. 23a) and maximum density (Fig. 23b). However, there is a decrease in the intensity, meaning that the amplitude of the oscillations shorten (because there is less movement), implying a reduction in energy and less density.

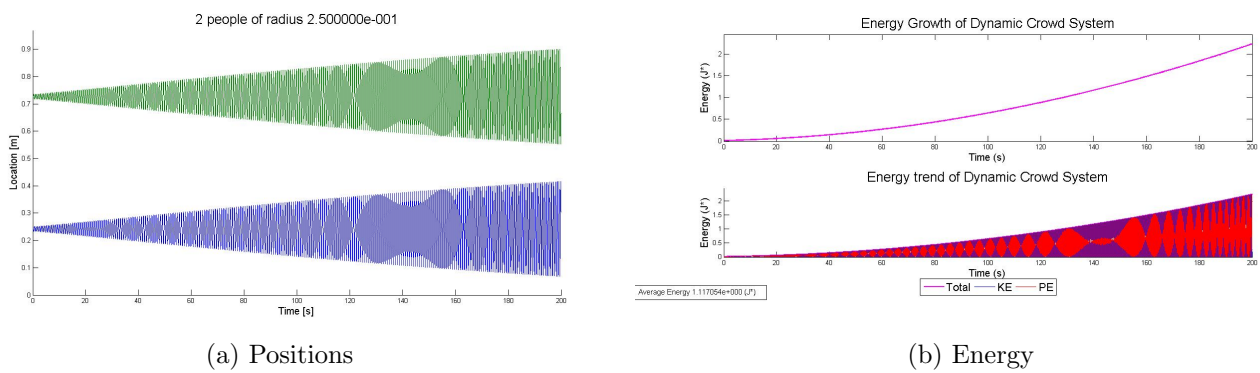


Figure 22: Position and energy plots for simulation 5

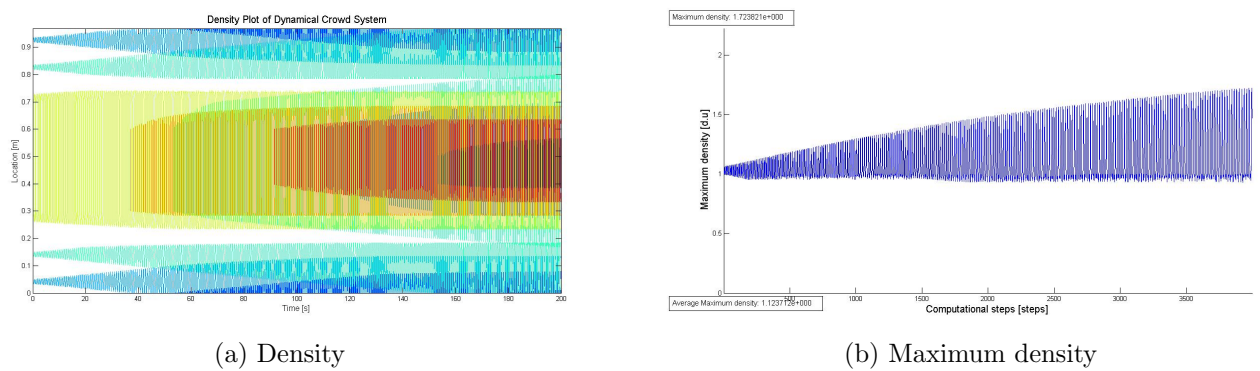


Figure 23: Density plots for simulation 5

Simulation 6

Initial configuration	Small Disturbance II
Slack	Yes
Mass configuration	Regular mass distribution
Pushing force	None
Time [s]	100

For the first time, in this simulation the initial configuration is switched to the Small Disturbance II. As it occurred in simulation 2, energy remains constant because the normal force is conservative (Fig. 24b). The oscillations are much different than in the previous simulation, and seem to be quasi-periodic (Fig. 24a). Besides, there is an obvious dependence of the positions of the initial configuration, present not only in the first seconds. Density also does not increase over time in the long-term. We can observe this quasi-periodic behavior in both density plots so that there is no evolution over time (Figs. 25a and 25b).

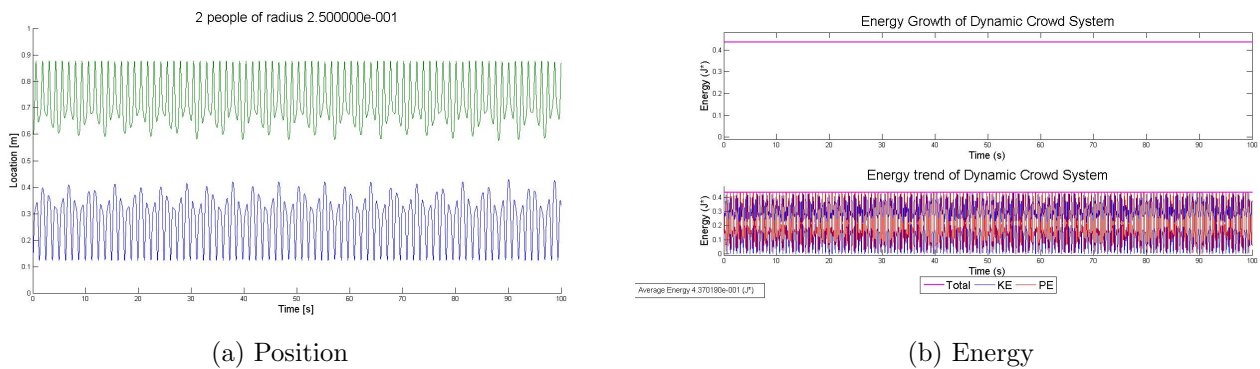


Figure 24: Position and energy plots for simulation 6

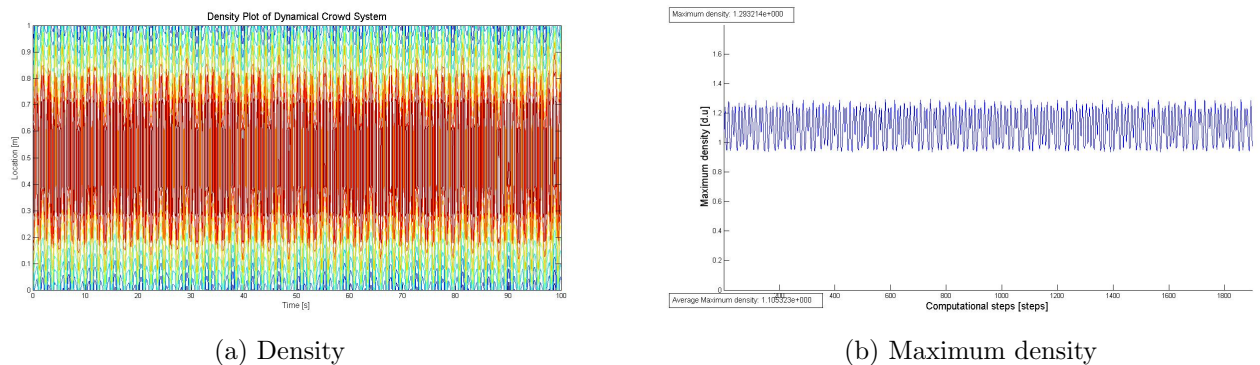


Figure 25: Density plots for simulation 6

Simulation 7

Initial configuration	Small Disturbance II
Slack	Yes
Mass configuration	Massive Extreme Configuration
Pushing Force	Anti-plastic
Time	100

Now, we introduce a different mass configuration (person one has 2 mass units and person two has 1 mass unit). We observe how person one although there is an increment of the amplitude its oscillations, this increment is reduced if we compare to the case of regular mass distribution whereas person two increases it (Fig. 26a). It seems physically rational that a pedestrian with less mass moves more than a heavy pedestrian as it is harder to move someone whose weight is larger. Total energy still increases in the long-term because it is induced by the introduction of the anti-plastic force, although the reached values are below the ones obtained in the regular mass distribution case (Fig. 26b). Density plots follow the same tendency, in spite of the fact that the reached values are lower, as it happens with relation to the total energy, that in the previous case (Figs. 27a and 27b).

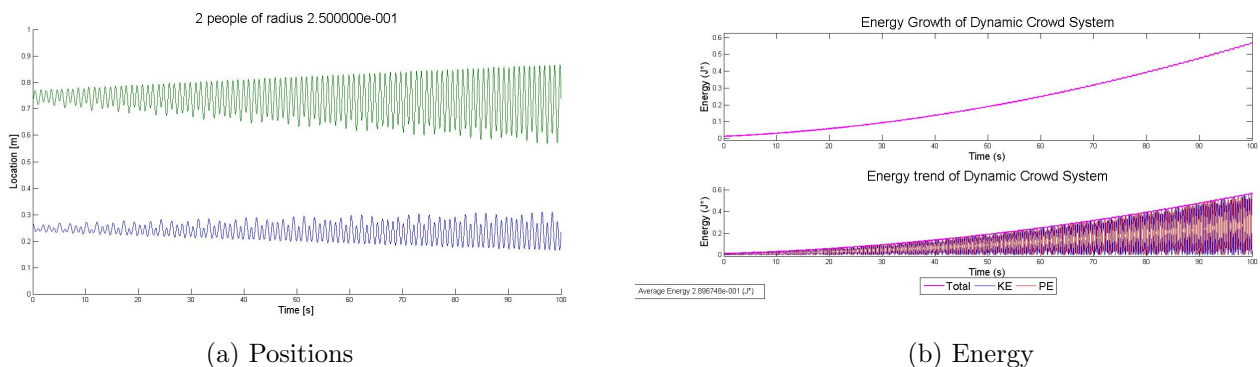


Figure 26: Position and energy plots for simulation 7

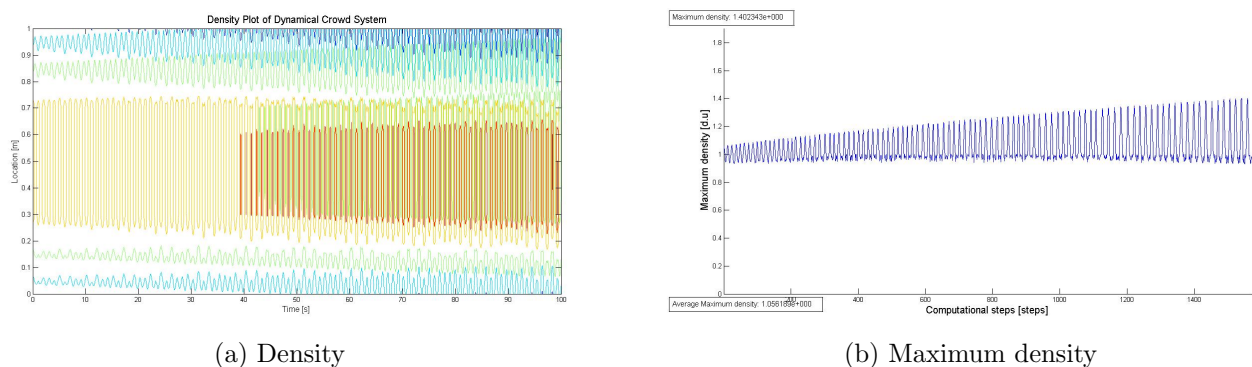


Figure 27: Density plots for simulation 7

Simulation 8

Initial configuration	Small Disturbance II
Slack	Yes
Mass configuration	Regular mass distribution
Pushing force	Plastic
Time [s]	100

In contrast with what we observe in previous simulations, the amplitude of the pedestrian's oscillations decrease over time till the system stabilizes (Fig. 28a). In this case, as predicted, the plastic pushing force reduces the energy (Fig. 28b). Similarly, the density decreases over time as well as the maximum density (Figs. 29a and 29b). Furthermore, it seems that there is a direct relation among energy, density and amplitude of the oscillations. This hypothesis will be verified in the case $n=50$.

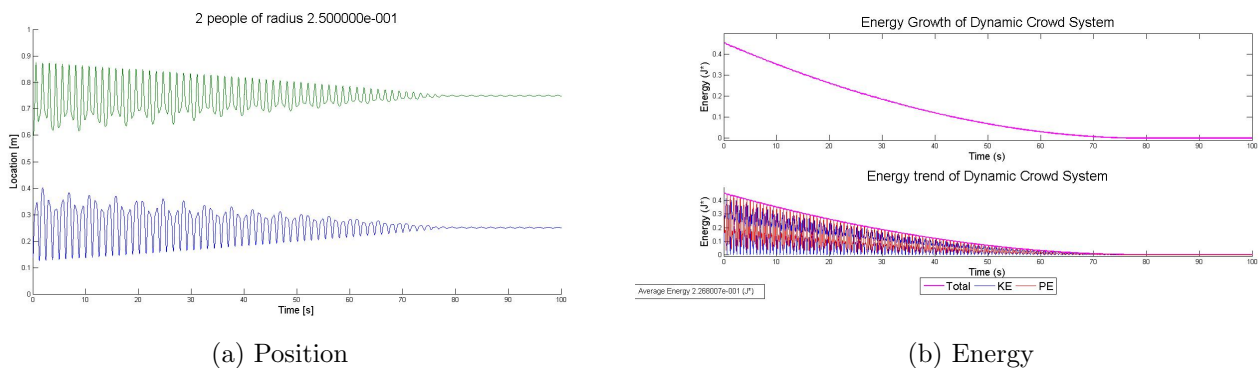


Figure 28: Position and energy plots for simulation 8

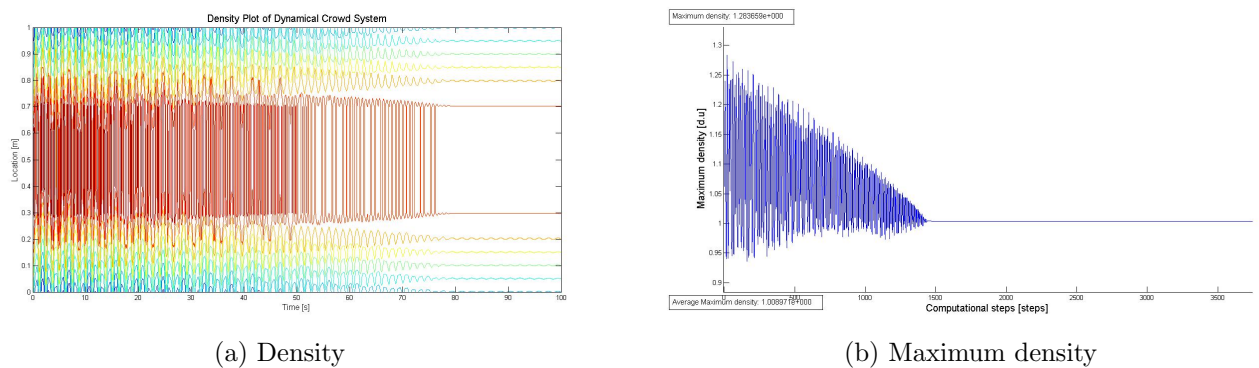


Figure 29: Density plots for simulation 8

7.2.2 Simulations with 50 pedestrians

In this section, simulations with the case $n = 50$ are introduced. We have chosen this value because it is large enough to show the behavior of the model in case of

a large number of people, and, at the same time, it does not induce computational issues related with long simulation times.

Simulation 9

Initial configuration	No overlap
Slack	Yes
Mass configuration	Regular mass distribution
Pushing force	Anti-plastic
Time [s]	100

We start with the same configuration as in the experiments for two pedestrians, this is, $\Delta_i \leq 0 \forall i \in \{L, R, 1, \dots, n-1\}$. The first simulation with 50 pedestrians shows us that, in case there is no overlap, all pedestrians remains in their position (Fig. 30a). This result verifies that the forces works properly when $\Delta_i \leq 0, \forall i \in \{L, R, 1, \dots, n-1\}$. As in simulation 1, total energy (Fig. 30b), density (Fig. 31a) and maximum density (Fig. 31b) remains constantly zero.

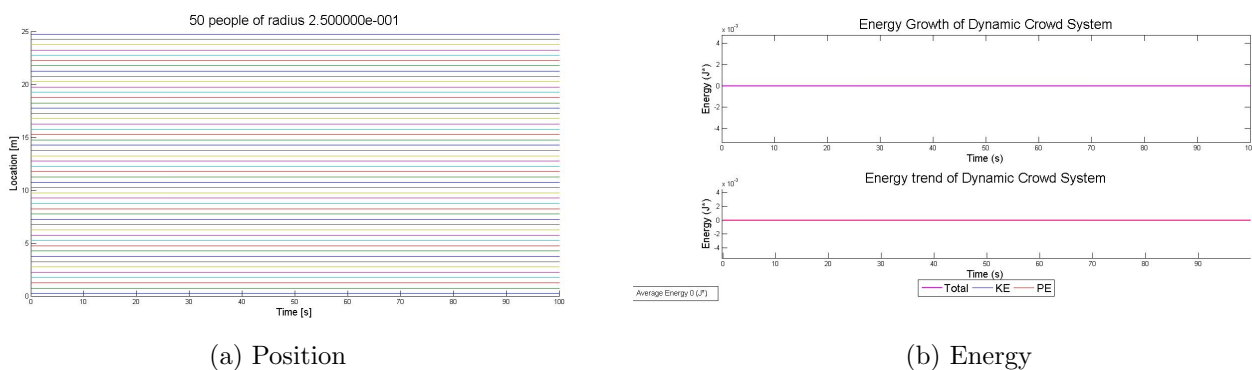


Figure 30: Position and energy plots for simulation 9

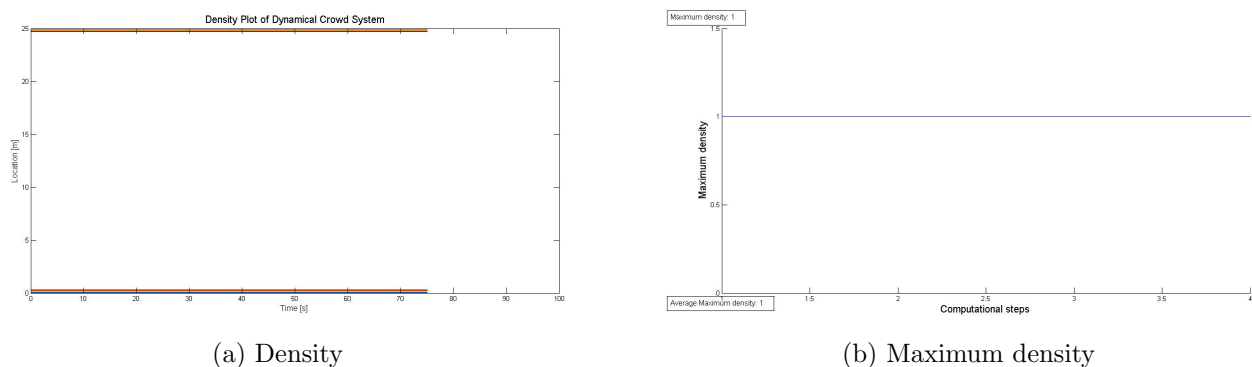


Figure 31: Density plots for simulation 9

Simulation 10

Initial configuration	Bell curve
Slack	Yes
Mass configuration	Regular mass distribution
Pushing force	None
Time [s]	200

In the second simulation with $n = 50$ a new initial configuration is set: the bell curve (see Fig. 32).

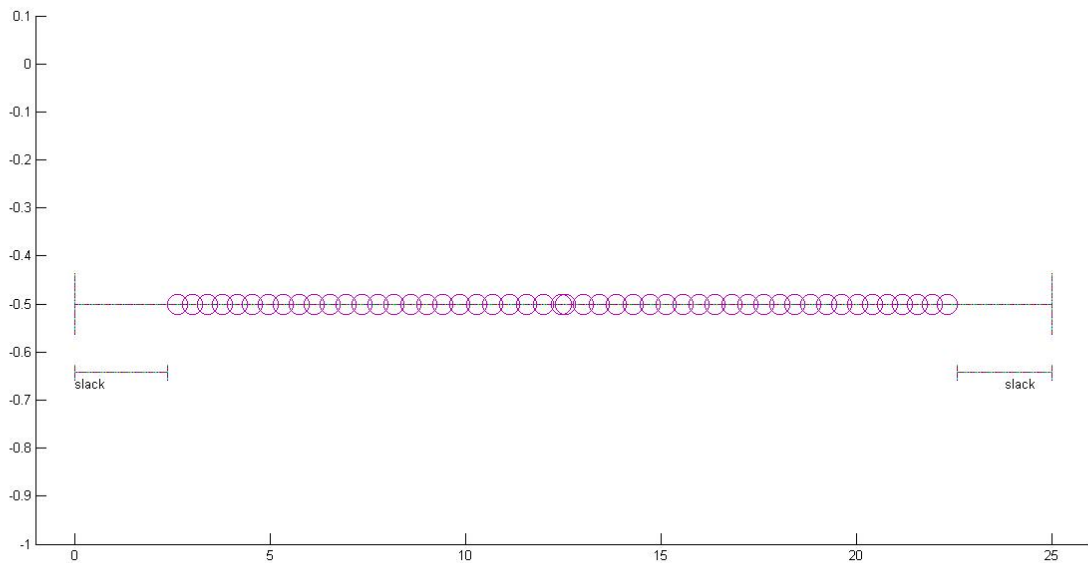


Figure 32: Bell curve with slack

As well as in simulations 2 and 7, energy remains constant because the normal force, which is the only one that plays a role in this case, is conservative (Fig. 33b). The position figure shows the dense center of the distribution spreading out until the boundaries are reached (Fig. 33a). Looking closely, pulse waves can be seen traveling between the walls. As time increases, noise from other collisions dilute the appearance of these pulses. Likewise, the density plot provides a clearer visual representation on how these wave propagate (Fig. 34a). The density peaks travel along the pulses and appear red in the density figure. However, the density peaks do not grow over time neither in number nor in intensity as we observe in Fig. 34b.

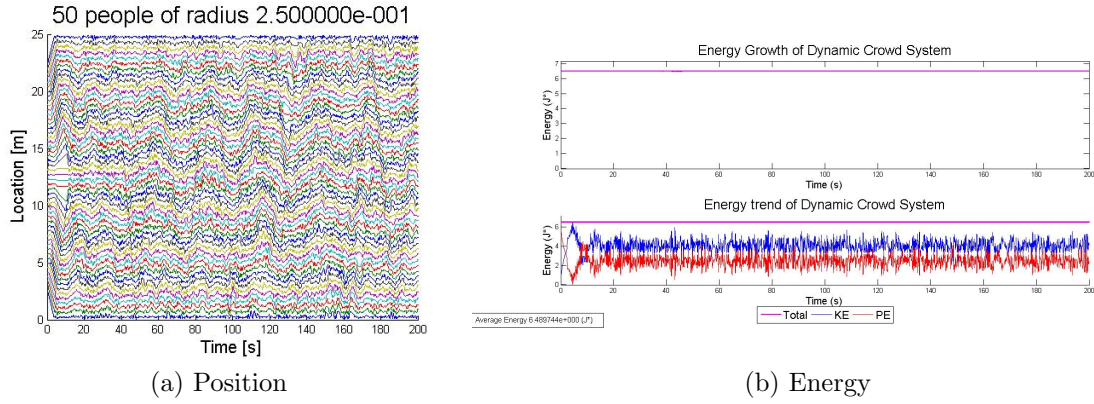


Figure 33: Position and energy plots for simulation 10

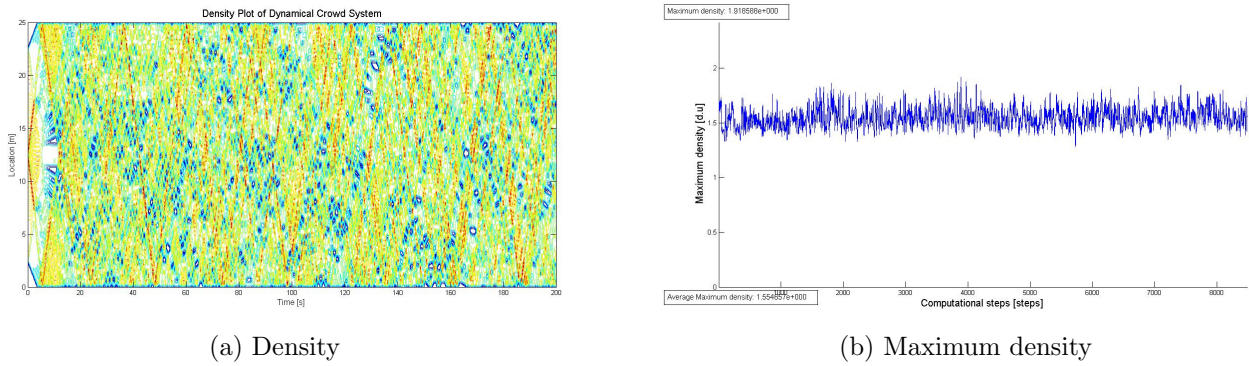
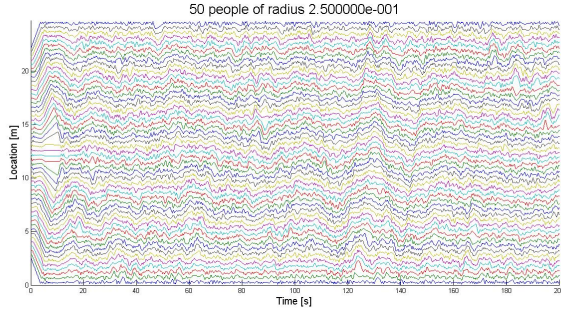


Figure 34: Density plots for simulation 10

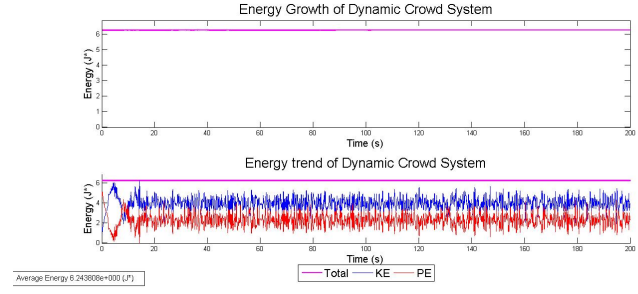
Simulation 11

Initial configuration	Bell curve
Slack	No
Mass configuration	Regular mass distribution
Pushing force	None
Time [s]	200

In this simulation, as in the case of two pedestrians, the difference between slack and reduced slack is not significant. It is found out that the behavior is pretty similar in both scenarios being able to observe the existence of pulse waves (Fig. 35a). While the value of the average energy is barely higher in the previous simulation (Fig. 35b), the average maximum density is slightly higher in this case (Fig. 36b). Then, it is concluded that in our model small differences in the length of the interval does not change significantly the final result.

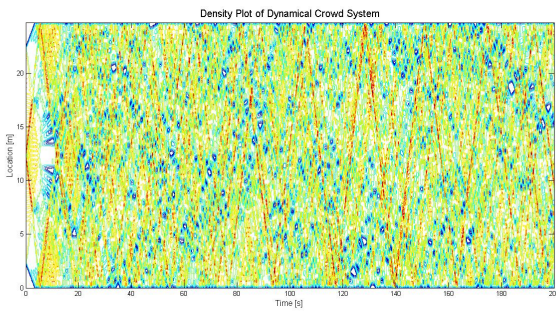


(a) Position

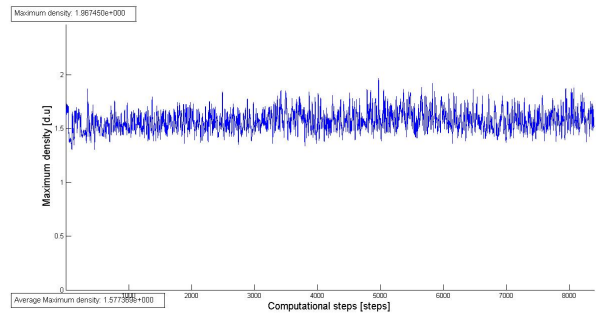


(b) Energy

Figure 35: Position and energy plots for simulation 11



(a) Density



(b) Maximum density

Figure 36: Density plots for simulation 11

Simulation 12

Initial configuration	Alternating disturbance
Slack	Yes
Mass configuration	Regular mass distribution
Pushing force	None
Time [s]	100

In the fourth scenario, the alternating disturbance configuration is introduced in the model as the initial set up (see Fig. 37 for a visual representation of this configuration).

We can easily see the initial wave which is very different from the result obtained with the bell curve configuration. Thus, there is a strong dependency of the initial configuration as also noticed in the two pedestrian case. This strong dependency is also found when the existence of solution for our system of equations is theoretically studied (see Appendix 12.2). The alternating initial configuration without the presence of any force leads to 'calm' behavior in the first 40 to 60 seconds and then, unpredictable behavior follows. This profile leads to more fluctuations in the middle and more squishing against the walls (Fig. 38a). This situation is more stable and

less dangerous than the bell curve at least at the beginning. As mentioned previously, the energy remains constant because the normal force is conservative (Fig. 38b). It is also interesting to observe how the density growth seems to be related with the waves too, as we detected in the previous cases (Fig. 39a). Unexpectedly, density peaks do not occur along these pulse waves formed in the beginning. Instead, minima in density occur along these pulses. The highest density peaks appears at the end of the simulation as a consequence of this unpredictable behavior. This increment in the density is also observed in the maximum density plot (Fig. 39b).

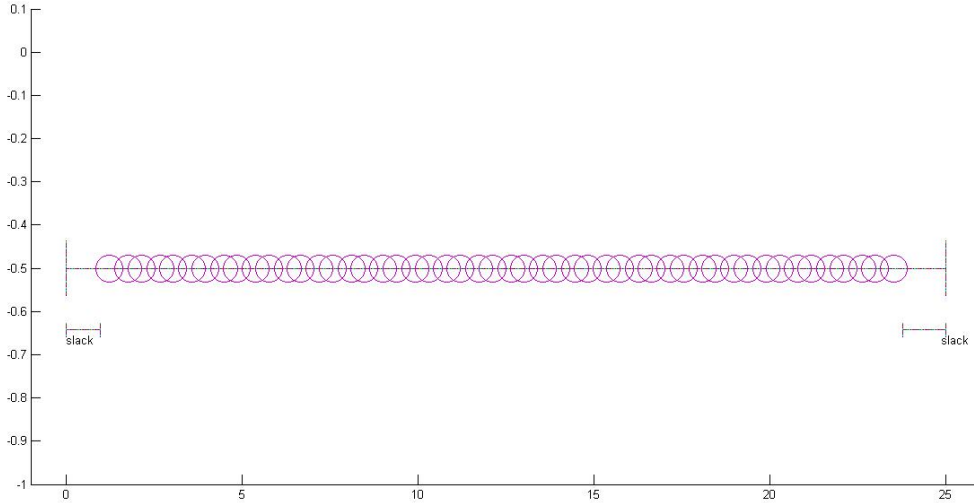
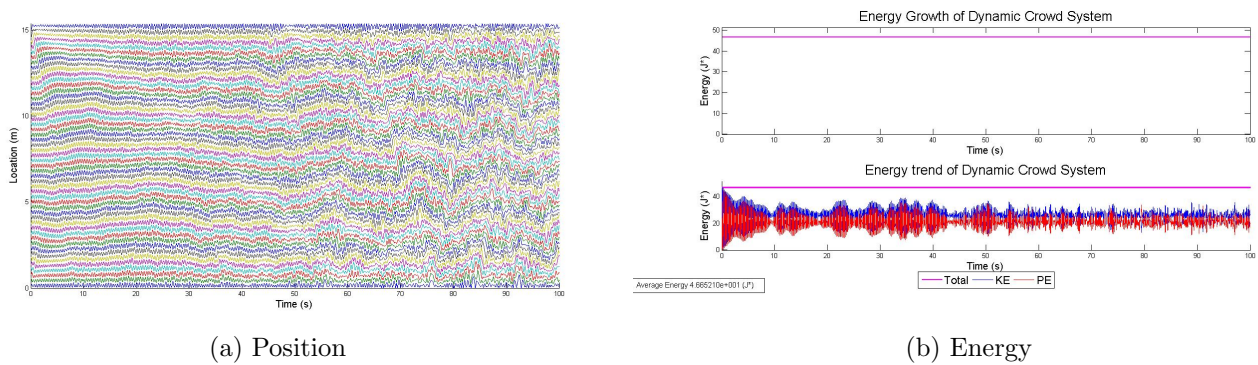


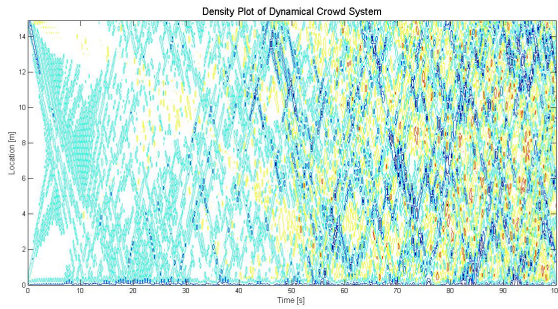
Figure 37: Alternating disturbance with slack



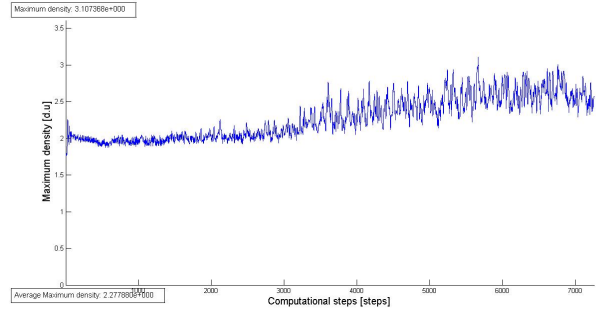
(a) Position

(b) Energy

Figure 38: Position and energy plots for simulation 12



(a) Density



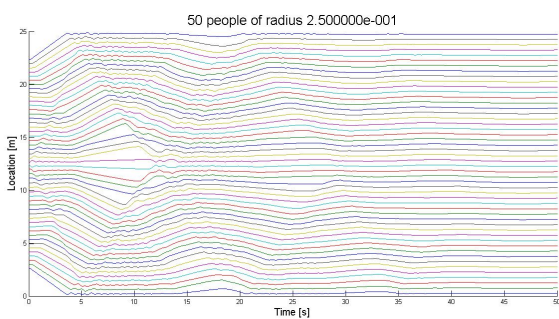
(b) Maximum density

Figure 39: Density plots for simulation 12

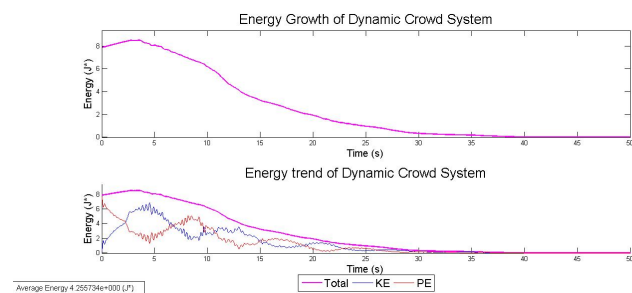
Simulation 13

Initial configuration	Bell curve
Slack	Yes
Mass configuration	Regular mass distribution
Pushing force	Heaviside
Δ_0	0.001
Time [s]	100

In this simulation we consider the Heaviside pushing force for first time. We can easily observe the initial wave caused by the given configuration and how it disappears when the system stabilizes like it happened previously in the case of the plastic one (Fig. 40a). Probably this stabilization is caused by the pushing force which also leads to a decrease of the energy, although in this case it grows in the first seconds, fact which could be induced by the initial configuration (Fig. 40b). In the density figures we can identify the high density peaks along the pulses of the initial wave which disappear whenever the system stabilizes (Figs. 41a and 41b).

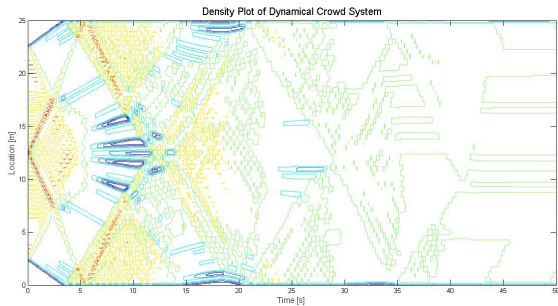


(a) Position

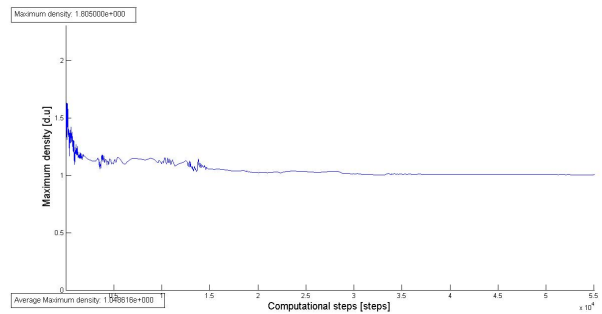


(b) Energy

Figure 40: Position and energy plots for simulation 13



(a) Density



(b) Maximum density

Figure 41: Density plots for simulation 13

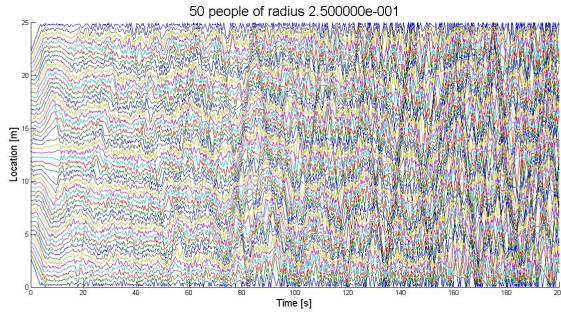
Simulation 14

Initial configuration	Bell curve
Slack	Yes
Mass configuration	Regular mass distribution
Pushing force	Anti-plastic
Time [s]	200

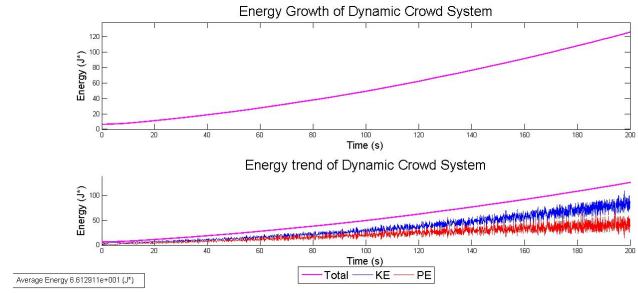
Let's consider what happens in case the energy increases over time in the long term. In order to carry out this task, the Heaviside pushing force is substituted by the anti-plastic one. It is checked that the energy increases as it did in the two pedestrians case.

In this simulation, it is noticed how after about 80 seconds the movement grows and isolated high density peaks, not related with the waves, are found as it happened in the cases where the normal force was the only one acting or adding the Heaviside one. We are also able to detect those points thanks to the maximum density plots, which show us how the maximum density also increases over time in the long term (Fig. 43b).

If we compare these outputs with those coming from the same simulation without pushing forces (simulation 10), a similar pattern is revealed from the start but the pulse waves become more apparent over time rather than diluting as shown in Fig. 42a. The overall density reaches higher values but these values do not fluctuate much being isolated the high density peaks (Fig. 43a). The energy increases as well as in the two pedestrian case with the small oscillations (Fig. 42b), expected thanks to the equation (Fig. 28).

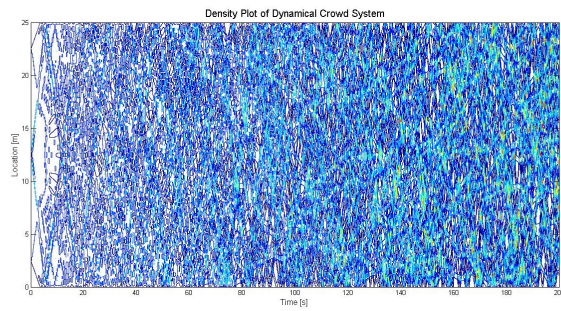


(a) Position

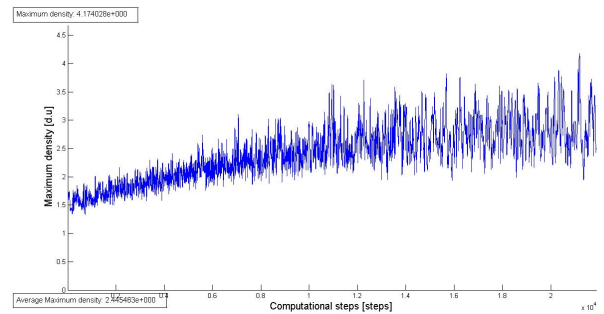


(b) Energy

Figure 42: Position and energy plots for simulation 14



(a) Density



(b) Maximum density

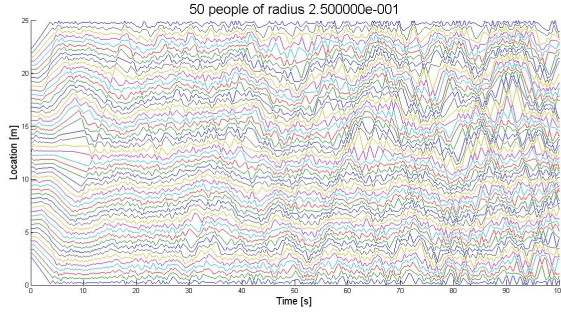
Figure 43: Density plots for simulation 14

Simulation 15

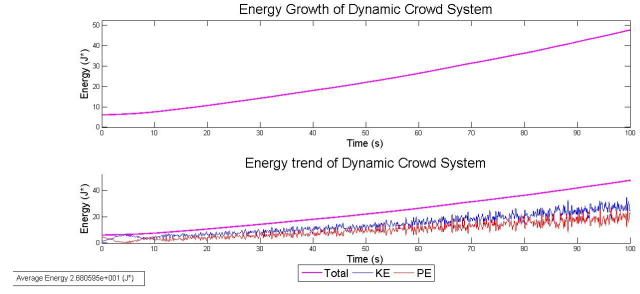
Initial configuration	Bell curve
Slack	Yes
Mass configuration	Massive center distribution
Pushing force	Anti-plastic
Time [s]	100

In this case, the last factor whenever the number of pedestrians is 50 is set: a different mass configuration.

The results of this simulation show a similar behavior of that case where every mass is equal to one (Fig. 44a). However, the total energy (Fig. 44b) and density (Figs. 45a and 45b) are slightly lower, so small differences in mass configuration just barely disturb the results. As this simulation is 100 seconds long instead of 200, no chaotic behavior is observed as previously. Therefore, it is possible to conclude that most dangerous moments may take place after enough time when there is more energy in the system, and consequently more higher density values and more oscillations of the maximum density. In this case, the high density peaks are easily observable in Fig. 45a and are not found to be related with pulse waves.

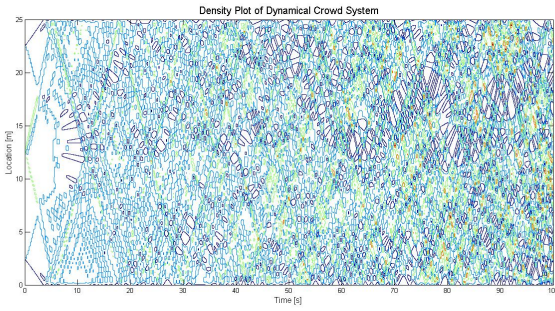


(a) Position

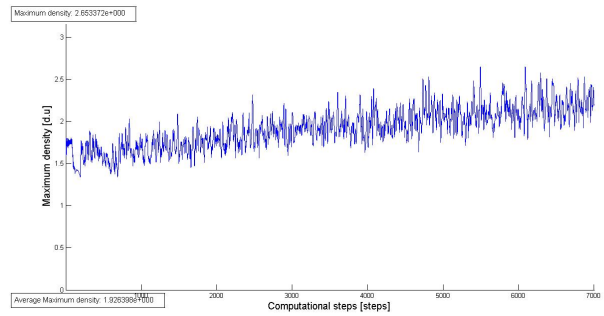


(b) Energy

Figure 44: Position and energy plots for simulation 15



(a) Density



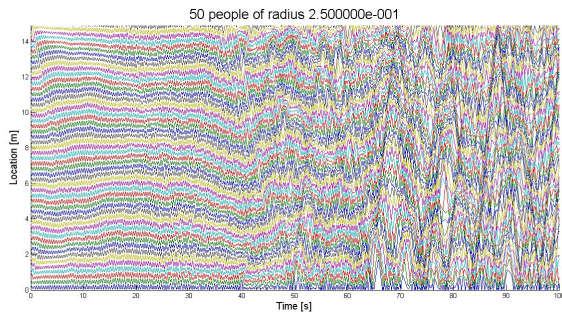
(b) Maximum density

Figure 45: Density plots for simulation 15

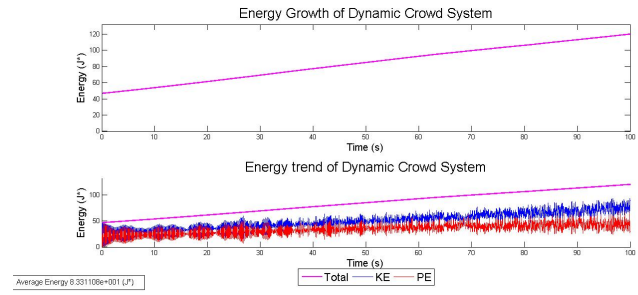
Simulation 16

Initial configuration	Alternating disturbance
Slack	Yes
Mass configuration	Regular mass distribution
Pushing force	Anti-plastic
Time [s]	100

At this point, the anti-plastic pushing force in the alternating configuration are introduced, producing results (Fig. 46a) quite similar in the first 40 seconds that in the previous case. However, after that time the result becomes completely unpredictable and isolated high density peaks not related to any wave are remarked (Fig. 48a). This behavior is a result of the introduction of a pushing force which increases the energy and the density (Figs. 46b, 48a and 48b). The fact that random behavior appears earlier than in the previous case is due to the initial configuration that again plays an important role in the resulting positions. Once again, we can observe the energy increment when the anti-plastic pushing force is used, looking closely at the total energy plot in Fig. 47. Furthermore, we find again the expected oscillations in the total energy as well as the growth of the maximum density. Yet, in this scenario it seems to rise at a lower pace.



(a) Position



(b) Energy

Figure 46: Position and energy plots for simulation 16

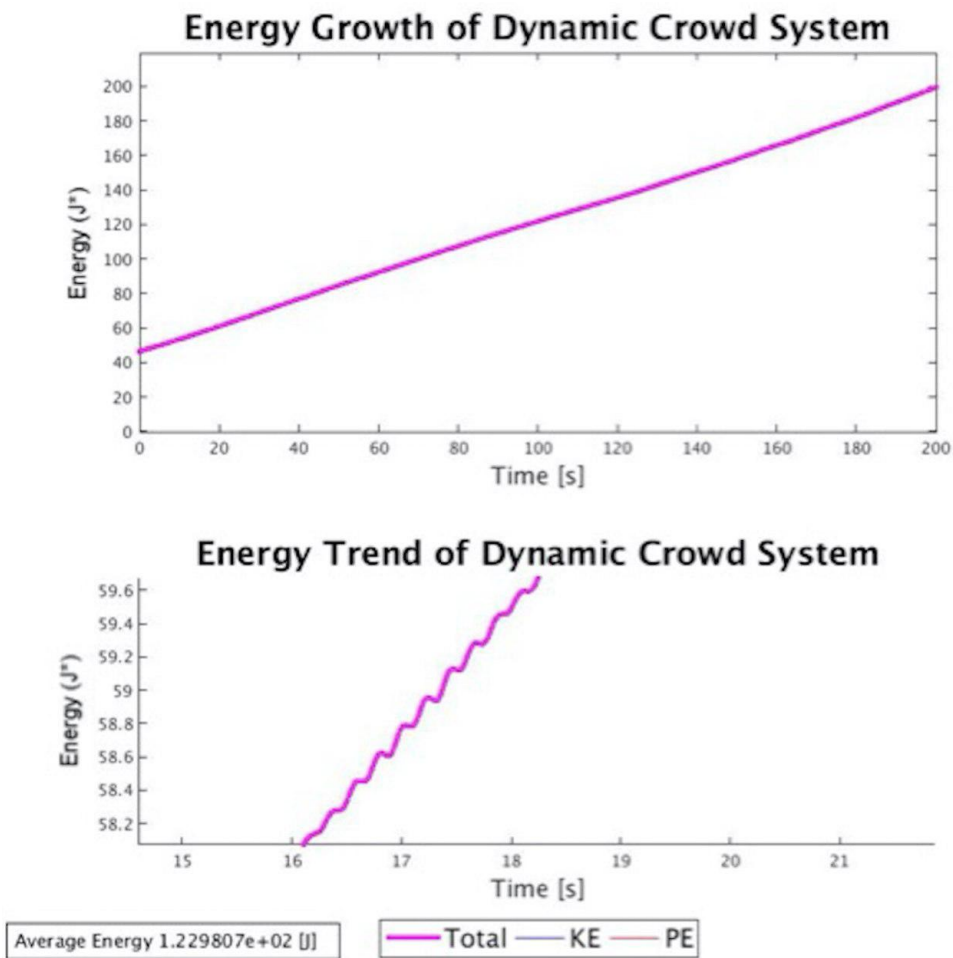
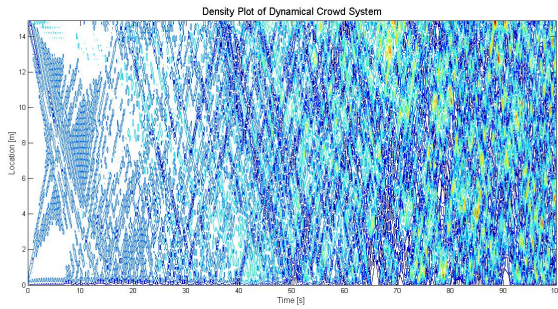
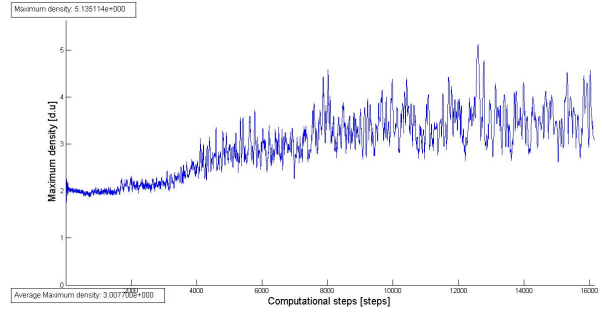


Figure 47: Zoom of the energy to observe the oscillations



(a) Density



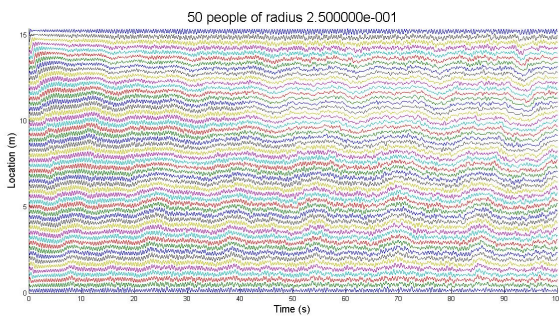
(b) Maximum density

Figure 48: Density plots for simulation 16

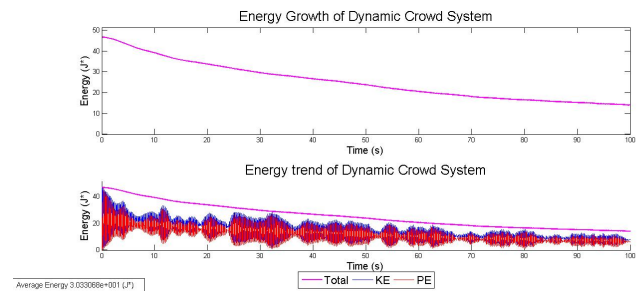
Simulation 17

Initial configuration	Alternating disturbance
Slack	Yes
Mass configuration	Regular mass distribution
Pushing force	Heaviside
Δ_0	0.001
Time [s]	100

Substituting the anti-plastic force by the Heaviside one with $\Delta_0 > 0$, we obtain a small decrease in the energy (Fig. 49b) that leads to a more stable configuration, in which there are always tiny oscillations (Fig. 49a), but there are neither high density peaks (Fig. 50a) nor huge displacements. The stability of this scenario is also found in the density plots, where the oscillations of the density are not significant if we compare with the previous ones (Fig. 50b).

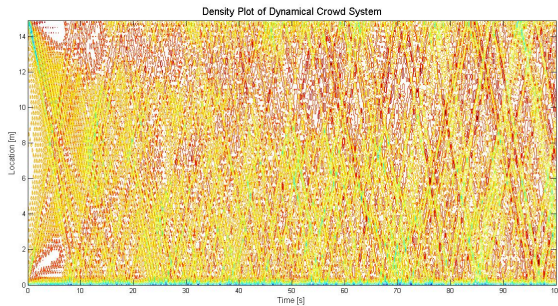


(a) Position

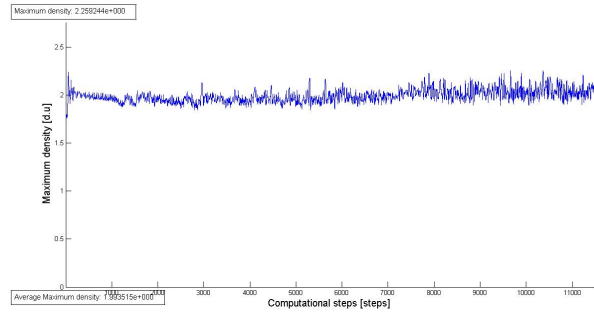


(b) Energy

Figure 49: Position and energy plots for simulation 17



(a) Density



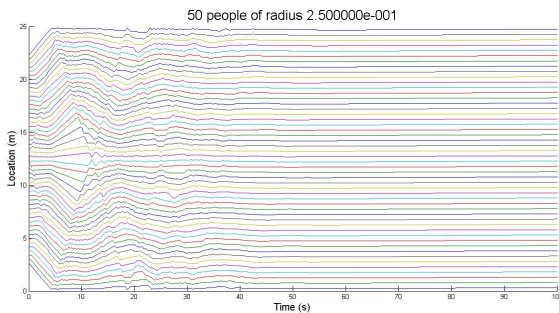
(b) Maximum density

Figure 50: Density plots for simulation 17

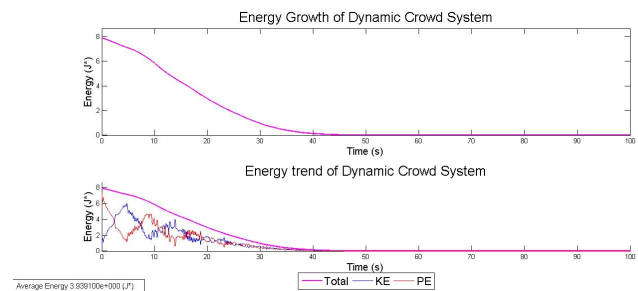
Simulation 18

Initial configuration	Bell curve
Slack	Yes
Mass configuration	Regular mass distribution
Pushing force	Plastic
Time [s]	100

Finally, the plastic pushing force is introduced in simulations with 50 pedestrians. We can observe the initial wave induced by the positions configuration at the beginning of Fig. 51a and how it disappears over time when the system stabilizes. Another consequence is the appearance of density peaks only along the pulse waves and the dissipation of the density whenever there are no pulse waves (Fig. 52a). In fact, if we observe the maximum density plot (Fig. 52b) there is a fast decrease at the beginning and, after that, it remains constant and close to 1 as the configuration is stable. Moreover, as mentioned previously in the two pedestrians case, the energy decreases and it is almost constant in the long term (Fig. 51b). This decrease is faster than in the Heaviside case as in this scenario the energy tends to zero while in the Heaviside one does not.

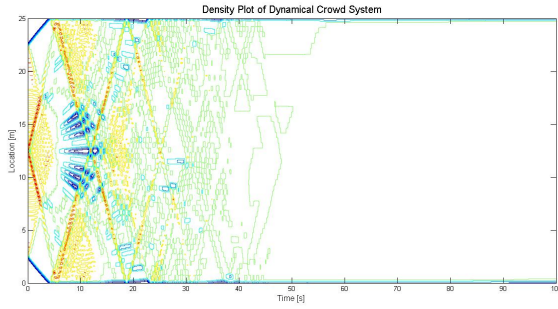


(a) Position

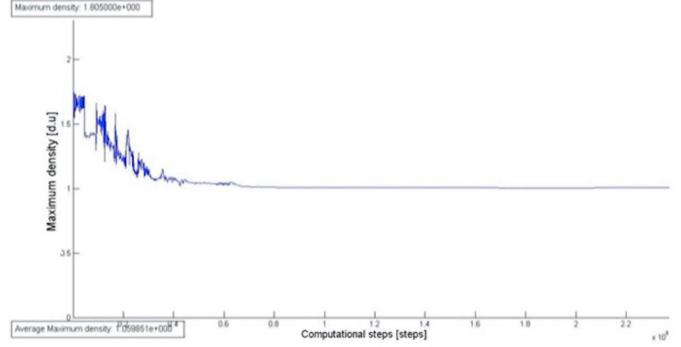


(b) Energy

Figure 51: Position and energy plots for simulation 18



(a) Density



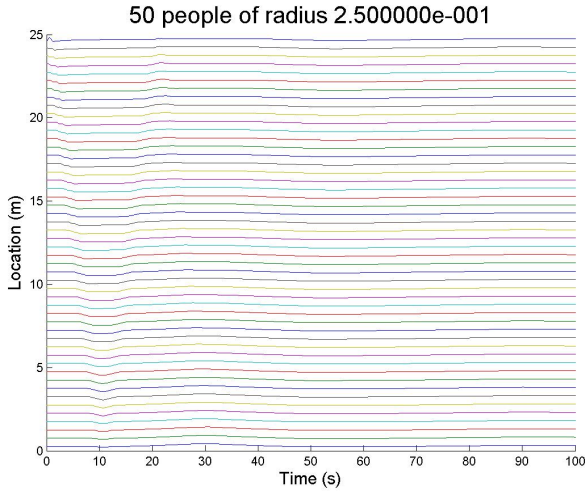
(b) Maximum density

Figure 52: Density plots for simulation 18

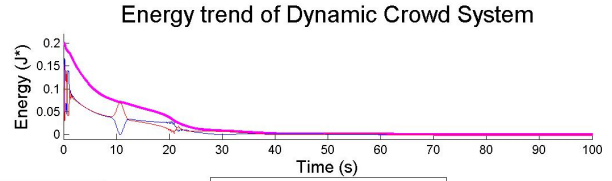
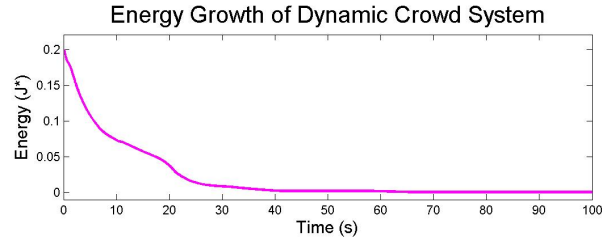
Simulation 19

Initial configuration	Small disturbance II
Slack	Yes
Mass configuration	Regular mass distribution
Pushing force	Plastic
Time [s]	100

Hereafter, in the last $n = 50$ pedestrians simulation, the initial configuration is the small disturbance II, being $\Delta_{n-1} > 0$, $\Delta_i = 0$, $\forall i \neq n - 1$. Similarly to what observed results from previous simulations, there is strong dependence on the initial configuration at the beginning of the simulation (it is better observed in the density plot placed at Fig. 54a through the pulse wave). Still, after few seconds the system stabilizes as in other simulations in which we have included the plastic pushing force (Fig. 53a). This stabilization is caused by the decrease of the energy which is induced by the plastic force too (Fig. 53b). As it has been already pointed out, the density plot depends strongly on the initial configuration. In the first seconds it is easily observed the wave caused by the initial configuration as the higher density is found along the pulse wave. After that moment, there are almost no changes in density as the system is in quasi-equilibrium (Fig. 54a).



(a) Position

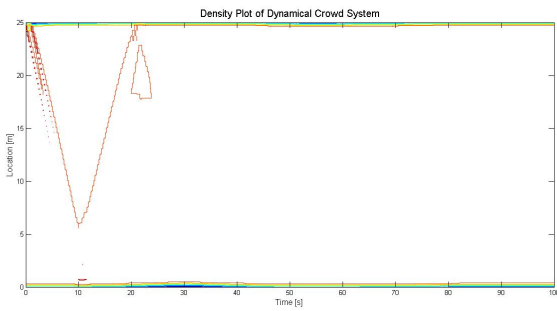


Average Energy $1.005078e-001$ (J*)

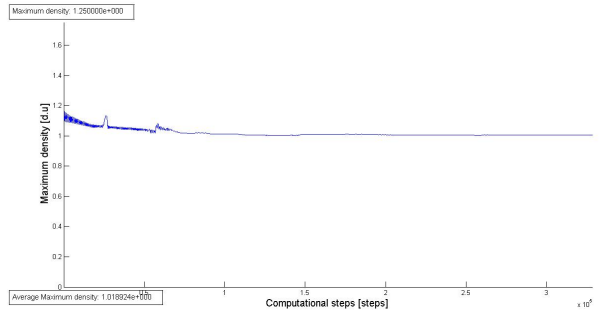
— Total — KE — PE

(b) Energy

Figure 53: Position and energy plots for simulation 19



(a) Density



(b) Maximum density

Figure 54: Density plots for simulation 19

7.2.3 Simulations with more than 50 pedestrians

Simulation 20

Initial configuration	Bell curve
Slack	Yes
Mass configuration	Regular mass distribution
Pushing force	Anti-plastic
Time [s]	200

This simulation represents the movement of 100 pedestrians and it corroborates what is observed in the case of 50 people, so we could generalize what we have concluded for n different people where n is big enough and the other conditions (such as length of the interval, slack, mass, etc.) remains constant. We remark that the same pulse waves stand in this simulation (Fig. 55a) as well as the oscillating increment

of the total energy (Fig. 55b), the isolated high density peaks (Fig. 56a) and the increment of the maximum density (Fig. 56b), analogously for the simulation for 50 pedestrians.

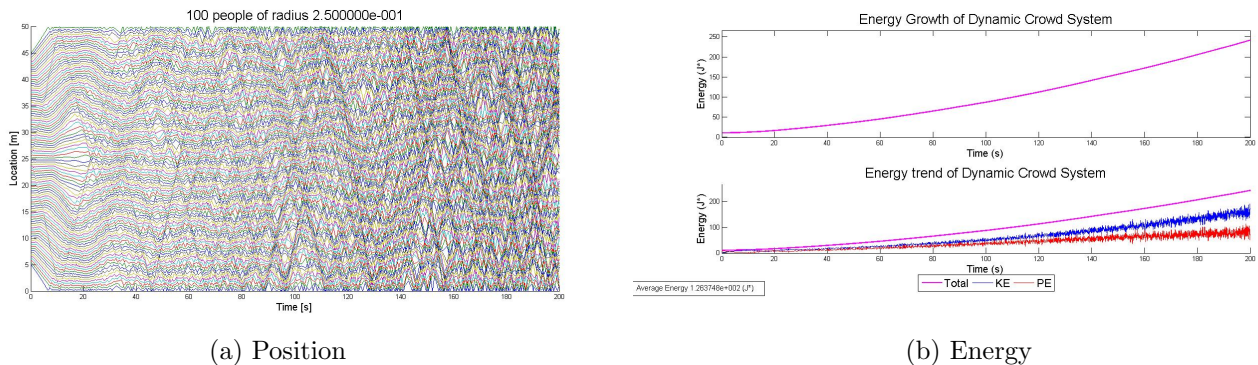


Figure 55: Position and energy plots for simulation 20

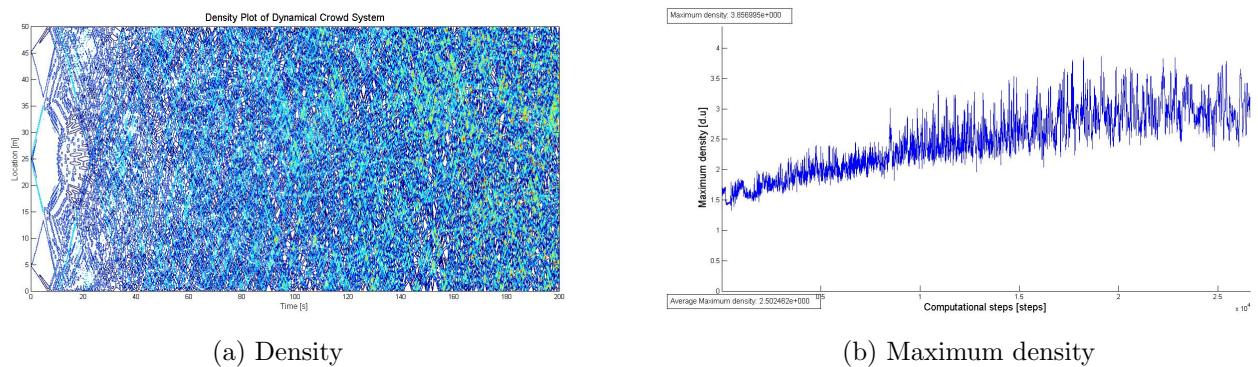


Figure 56: Density plots for simulation 20

7.3 Other observations

Once that some of the results of most important simulations have been presented in the section above, it is time to introduce further comments and observations based on the outputs of simulations that were neither selected nor mentioned before.

Firstly, simulations with $n = 2$ yield interesting behavior. In general, people in small disturbance configuration II oscillates with more amplitude than in small disturbance I with and without slack. Normal force cases show oscillations between constant upper and lower bounds while simulations with anti-plastic pushing force show an increment in the amplitude of the oscillations, caused by the definition of these pushing force that increases the energy of the system. In case of the Heaviside and plastic forces, the amplitude of the oscillations decrease, being more noticeable the reduction in the case of the plastic one. Small disturbance configuration I seems to be more stable than configuration 4 as there are no "peaks" which are observed

in configuration II.

With respect to the energy, the results obtained are the same as in the case of fifty pedestrians (mentioned below). Setting only the normal force, the total energy remains constant (because it is a conservative force). Anti-plastic pushing force induces an increment of total energy, with some small oscillations due to the construction of this pushing force, similar to an increasing exponential function. Yet, Heaviside and plastic forces cause a decrease of total energy. The main difference regarding the energy is that in the case of the plastic the total energy tends to zero fast while using the Heaviside one leads to a slow decrease.

The average energy is greater in small disturbance configuration II because the value of the potential energy at time 0 is higher (the overlaps are greater) and the movement is larger so that kinetic energy is greater than in configuration I. Besides, overlaps are greater in configuration II over time (not only at time 0) which leads to an increment of the potential energy and consequently, the total energy. Furthermore, it has been noticed that slack and energy are not apparently related.

In general, density grows from the walls to the middle symmetrically when both masses are equal or displaced in case that the masses are different similarly to Fig. 27a. The most important observation with respect to density is that it changes in time when pushing forces vary energy, for instance, increasing it such as the anti-plastic one or decreasing such as Heaviside and plastic forces. The relation between energy and density is direct, so the more energy the more density. Hence, forces which increase energy such as the anti-plastic one could explain high densities in crowds as densities grow to high levels whenever energy does it too.

Secondly, the case of $n=50$ does also offer interesting results. Wavy pulses are shown in almost every simulation independently of the forces used, being an important feature of the model. Additionally, it is observed how increments in total energy leads to higher densities and most times to unpredictable behavior.

On the one hand, the anti-plastic pushing force shows a rise in the number of pulse waves. As a consequence, the most unstable behavior occurs after the first 100 seconds. From this time and on, pulses period are so small that making almost impossible to distinguish them. The density is once again higher than in the previous case, but little information can be extracted only from these plots alone. On the other hand, adding the plastic pushing force make the energy decrease very fast stabilizing the system in few seconds, being able to find "high" density peaks only along the initial pulse wave.

Moreover, the use of the Heaviside pushing force reveals a similar pattern to the one observed in the case of the normal force alone. This characteristic is a nearly stable solution in which there is still oscillations and the highest density peaks are observed along the waves.

The energy of the 50-pedestrians systems is predictable as in the previous case of $n = 2$. They do not depend on the initial profiles nor whether the slack was provided in the long term while these factors can slightly influence in the short term. The energy mostly depends on the forces, mainly in the pushing ones, acting on the people. In the case of just a normal force energy was always constant. On the contrary, the use of anti-plastic pushing force always resulted in an oscillating increasing exponential function. In contrast, the plastic and Heaviside ones leads to an oscillating decreasing function in the long term as we also observed in the simulations of the previous section.

Finally, with respect to initial configurations, the main differences take place in the positions during the first seconds due to the fact that they induce diverse pulse waves, being more unstable the bell curve configuration.

8 Conclusions

In spite of the fact that most of behaviors shown previously were unpredictable, conclusions can still be extracted from this project. We have found that modeling human behavior proves to be difficult because patterns are not easily distinguishable in highly populated plots. In addition, configuration spaces where people reside at do not affect patterns in energy growth, only the extent to which they grow. To change patterns in energy growths, it is necessary to model the crowd with different forces. Regarding our model, the total energy depends on the pushing forces, fact that has been proved in equation 28.

Initial profiles mainly determine the dynamics at least at the beginning and consequently density distribution strongly depends on them as well. Pulse waves within crowds depend on where boundaries are located. Density extrema (maxima or minima according to the chosen initial conditions) occur most of the times along these pulses. However, density also depends on pushing forces. In fact, it increases over time only in case we introduce energy in the system, as it is easily observed in the simulations, and decrease whenever the energy is reduced. Therefore, there is a direct relation between energy and density.

In relation with energy it is important to remark that an increment in the energy leads to unstable behavior, pulse waves and high density isolated areas. These feature are exactly the ones we looked for when we introduced pushing forces in the model. Whereas, a reduction in the energy leads to a stable system. The empirical relation between energy and density and the proven relation between energy and density evidence that pushing forces in a crowd can induce high density peaks and then dangerous situations which was the main goal of this project.

Moreover, it seems that there also exists a relation among energy, position and overlaps. This relation is not theoretically proved although there are some empirical

evidences. In the cases with more amplitude in the oscillations of the position, the energy and the overlaps are also greater. In particular, anti-plastic pushing force leads to increments of energy and overlaps because people are increasing their amplitude of oscillation and getting closer, while Heaviside and plastic forces lead to the opposite result. In the cases where the only force is the normal one, people are not getting closer and the energy is bounded (constant in the case of only a normal force) as well as the overlaps.

9 Limitations of the model

The main limitation we find in our model is that simulations cannot be run in long periods of time due to software constraints. Due to this issue, we can run simulations with few people and easy (computationally speaking) initial configurations during few minutes, however, when we introduce a huge amount of people and a not simple configuration we only can simulate for few seconds. In fact, at this point, we only can obtain conclusions about the first minutes in an stampede and only make assumptions about what we think it will happen after that precise moment.

We expect that these problems could be solved using a different software, an optimized code or a better computer (most of the simulations have been run on my own computer; however, in order to reduce the time spent on running simulations, we have used ALTAMIRA Supercomputer²). For example, there are some simulations which are unable to be completed as the intern memory of MATLAB was not sufficient due to the length of the vectors of position and velocity.

Regarding the theoretical part of the model, the main problem is that we are not able to ensure the existence a solution, and in case it exists, that it is unique. We can only prove the last statement for easy scenarios and just locally. It is expected that this result could be translated to the general case; however, it is just a non-proved hypothesis.

Another important limitation is related with numerical calculations. By definition, the normal force tends to infinite as people get closer. Nevertheless, when two or more people are extremely close to each other they may change positions (an event which is not allow). Furthermore, it is not possible to come back to the original order as the normal force does not allow to change positions again. Then, there are simulations with very specific parameters and configurations (mainly when the constant parameters of the forces are big enough, the velocities are high and in opposite directions, which in this one dimensional model means with opposite sign, and configurations with people very close to each other). Latest adjustments on the value of the constants have helped to avoid this problem in most situations, however,

²We acknowledge Santander Supercomputacion support group at the University of Cantabria who provided access to the supercomputer ALTAMIRA Supercomputer at the Institute of Physics of Cantabria (IFCA-CSIC), member of the Spanish Supercomputing Network, for performing simulations/analyses.

it is possible that it happens under extreme conditions.

Besides, something that should be considered and that it is not included in this model because of its complexity (this is a simple model) is to "eliminate" the pedestrians who are placed in an emplacement where the density is very high (it is considered that 6 people/ m^2 is life threatening) and that are probably seriously injured or dead.

On the other hand, we are not taking into consideration the friction (it is somehow included in constant P , for example). Despite it could be easily introduced, we believe omitting it simplifies the equations so that it is easier to draw conclusion from the obtained results.

To conclude, the last limitation found is the mass configurations we have chosen are not significant for a high number of people and consequently we cannot draw conclusions in relation with mass. In order to solve this problem we should define new mass configurations and test them again.

10 Benefits of the model

From our point of view, the simplicity of this model is its most important accomplishment as it allows to change any input parameter, such as different length, mass, forces, number of pedestrians, . . . , without needing any further variation of the model as a whole. As a consequence of this property, a deep study of the understanding of the model can be performed easily by modifying those different factors in order to inspect the results straightforwardly.

Secondly, it introduces pushing forces as one of the possible reasons why crowd density rises a lot causing stampedes or other dangerous situations. We have found that pushing forces which increase energy cause an increment of the density of the system proving the previous hypothesis. In fact, thanks to the density measure, we are able to distinguish the areas where the risk of injuries or death is considerable. For example, this model could be used to prevent people to stay away from those dangerous areas when a stampede takes place.

Lastly, the wavy behavior observed in most of the simulations is also detected in real situations. These waves along with the high density areas are some of the features that encourage our motivation for stating that the model could hold for real situations such as the ones we have tested.

11 References

- [1] D. Helbing et al, "Simulation of Pedestrian Crowds in Normal and Evacuation Situations", *Peestr. Evac. Dyn.* **21**: 21–58 (2002)
- [2] D. Helbing et al, "Simulating Dynamical Features of Escape Panic", *Nature.* **407**: 487-490 (2000)
- [3] Prof. Dr. G. Keith Still webpage:
<http://www.gkstill.com/ExpertWitness/CrowdDisasters.html>
- [4] M. Moussaid et al, "How Simple Rules Determine Pedestrian Behavior and Crowd Disasters", *Proceedings of the National Academy of Sciences of the United States of America*, **108(17)**: 6884–6888 (2011)
- [5] R. Hughes, "A Continuum Theory for The Flow of Pedestrians", *Transportation Research Part B* **36(6)**: 507-535 (2002)
- [6] Human body weight article. Retrieved April 26, 2016 from https://en.wikipedia.org/wiki/Human_body
- [7] A. Treuille, S. Cooper, and Z. Popovic, "Continuum crowds", *ACM Trans. Graph.*, **25(3)**: 1160-1168 (2006)

12 Appendix

12.1 Dormand-Prince method

It is a Runge-Kutta based process to solve ordinary differential equations [8]. It is adaptive, as we will see, and it is based on Runge-Kutta solvers of order four and five [9]. Like other Runge-Kutta based methods it tries to solve the following Cauchy problem:

$$\dot{x} = f(t, x), \quad x_0 = x(t_0) \quad (34)$$

First, it starts with the Runge-Kutta method of order four:

It takes a size-step $h > 0$, the time step. Then:

$$t_{i+1} = t_i + h$$

In order to compute x_{i+1} (approximate value of the solution x at the point t_{i+1}) it computes several scalars ($k_1, k_2, k_3, k_4, k_5, k_6, k_7$) that are the derivatives (slopes) at different points. The definition of these scalars, the computation of x_{i+1} (the weight of each scalar) and the adaptive process to choose an optimal time step are what make it different from the other methods.

In Dormand-Prince method the coefficients are obtained in the following way:

$$k_1 = hf(t_i, x_i) \quad (35)$$

$$k_2 = hf\left(t_i + \frac{h}{5}, x_i + \frac{k_1}{5}\right) \quad (36)$$

$$k_3 = hf\left(t_i + \frac{3h}{10}, x_i + \frac{3k_1}{40} + \frac{9k_2}{40}\right) \quad (37)$$

$$k_4 = hf\left(t_i + \frac{4h}{5}, x_i + \frac{44k_1}{45} - \frac{56k_2}{15} + \frac{32k_3}{9}\right) \quad (38)$$

$$k_5 = hf\left(t_i + \frac{8h}{9}, x_i + \frac{19372k_1}{6561} - \frac{25360k_2}{2187} + \frac{64448k_3}{6561} - \frac{212k_4}{729}\right) \quad (39)$$

$$k_6 = hf\left(t_i + h, x_i + \frac{9017k_1}{3168} - \frac{355k_2}{33} - \frac{467328k_3}{5247} + \frac{49k_4}{176} - \frac{5103k_5}{18656}\right) \quad (40)$$

$$k_7 = hf\left(t_i + h, x_i + \frac{35k_1}{384} + \frac{500k_3}{1113} + \frac{125k_4}{192} - \frac{2187k_5}{6784} + \frac{11k_6}{84}\right) \quad (41)$$

These coefficients are computed in such a way that they can be used in the Runge-Kutta method of order 4 and in the one of order 5 reducing the number of function evaluations to 7 (instead of 14).

Afterwards we compute x_{i+1} using the method of order 4:

$$x_{i+1} = x_i + \frac{35k_1}{384} + \frac{500k_3}{1113} + \frac{125k_4}{192} - \frac{2187k_5}{6784} + \frac{11k_6}{84} \quad (42)$$

Second we calculate a corrected value of x_{i+1} , which we are going to recall as \hat{x}_{i+1} , using a Runge-Kutta method of order five:

$$\hat{x}_{i+1} = x_i + \frac{5179k_1}{57600} + \frac{7571k_3}{16695} + \frac{393k_4}{640} - \frac{92097k_5}{339200} + \frac{187k_6}{2100} + \frac{k_7}{40} \quad (43)$$

To obtain the optimal next size-step we compute the difference between x_{i+1} and \hat{x}_{i+1} , which is considered the error in x_{i+1} :

$$|\hat{x}_{i+1} - x_{i+1}| = \left| \frac{71k_1}{57600} - \frac{71k_3}{16695} + \frac{71k_4}{1920} - \frac{17253k_5}{339200} + \frac{22k_6}{525} - \frac{k_7}{40} \right| \quad (44)$$

Let $\epsilon > 0$ be the tolerance, the optimal time interval, h_{opt} is calculated as

$$h_{opt} = h \cdot s \quad (45)$$

where h is the previous time step interval and s is computed as

$$s = \left(\frac{\epsilon h}{2|\hat{x}_{i+1} - x_{i+1}|} \right)^{\frac{1}{5}} \quad (46)$$

When the difference between x_{i+1} and \hat{x}_{i+1} is big enough, the solution will probably oscillate abruptly in that area so it is necessary to decrease the time step ($s < 1$) to obtain a more accurate solution. On the other hand, if x_{i+1} and \hat{x}_{i+1} are close enough, the solution is likely to be smooth in that area and there is no need to reduce the time step, being $s \geq 1$.

12.2 A preliminary study about existence and uniqueness of solution of our ODE's system with discontinuous terms

The analysis of existence and uniqueness of solutions for our problem is not an easy task. Each equation depends on six variables $x_i, x_{i+1}, x_{i-1}, \dot{x}_i, \dot{x}_{i+1}, \dot{x}_{i-1}$ and it is related with the previous and the following one (this fact adds four more variables, $x_{i-2}, x_{i+2}, \dot{x}_{i-2}$ and \dot{x}_{i+2}). Moreover, there are discontinuous functions such as the pushing forces and the points where they are not continuous depends on the relations of the ten previous variables. It is clearly not an standard ODE system and it should be analyzed carefully. For those reasons, we find that fully studying the existence and uniqueness of solutions is out of the level of this project and furthermore it is not one of our main goals. However, this part is important for the validity of our model, so we are going to prove that there is a unique local solution for our problem at least under some particular conditions.

An important remark at this point is that if the initial conditions are not discontinuity points for the functions defining the ODE and the branch which satisfies the initial condition has a unique solution, then the whole problem has a unique local (at least) solution. We will see that sometimes there is a problem if the initial conditions are discontinuity points as in our system of ODEs.

Let's start with some examples similar to our problem to show all the possibilities that could appear (no solution, multiple solutions or unique solution).

Let's consider the following Cauchy's problem

$$\begin{cases} \ddot{x}(t) = f(x(t), \dot{x}(t)) \\ x(0) = 2, \quad \dot{x}(0) = 0, \end{cases} \quad (47)$$

where

$$f(x, y) := \begin{cases} x & \text{if } x > 0 \wedge y > 0 \\ 4(x - 1) & \text{if } x > 1 \wedge y < 0 \\ 0 & \text{otherwise} \end{cases}$$

Rewriting the ODE of 47 as a first order ODE system, we can deduce that the solution $x(t)$ is going to be C^1 and C^2 piecewise. We also observe that f is discontinuous at points of the form $(x, 0)$ with $x > 0$, $x \neq 1$, $x \neq \frac{4}{3}$.

In order to find the solutions we consider each branch of the system that we rewrite in following way:

$$\ddot{x}(t) = x(t), \quad x(0) = 2, \quad \dot{x}(0) = 0. \quad (48)$$

$$\ddot{x}(t) = 4(x(t) - 1), \quad x(0) = 2, \quad \dot{x}(0) = 0. \quad (49)$$

$$\ddot{x}(t) = 0, \quad x(0) = 2, \quad \dot{x}(0) = 0. \quad (50)$$

It is easy to deduce that the solution of problem (48) is:

$$x(t) = 2\cosh(t) \quad (51)$$

The solution of (49) is:

$$x(t) = \cosh(2t) + 1 \quad (52)$$

And finally the solution of (50) is:

$$x(t) \equiv 2 \quad (53)$$

We can construct different solutions of (47) by using combinations of the previous ones, this is, by copying and pasting the solutions of the different branches according to the requested conditions, for example:

$$x(t) \equiv 2$$

$$x(t) = \begin{cases} 2\cosh(t) & \text{if } t \geq 0 \\ 2 & \text{if } t < 0 \end{cases}$$

$$x(t) = \begin{cases} 2 & \text{if } t \geq 0 \\ \cosh(2t) + 1 & \text{if } t < 0 \end{cases}$$

Then, it is clear that this problem has several solutions.

If we change the initial conditions to $x(0) = 1$ and $\dot{x}(0) = 1$ (f is continuous at $(1,0)$), then we consider the following problem:

$$\begin{cases} \ddot{x}(t) = f(x(t), \dot{x}(t)) \\ x(0) = 1, \dot{x}(0) = 1. \end{cases} \quad (54)$$

Clearly, the solution in this case is $x(t) = e^t, \forall t \geq 0$. Furthermore, as $\dot{x}(t) = e^t > 0, \forall t \geq 0$ the solution does not leave the first branch, obtaining a global unique solution.

Another example leads to a completely different situation. Let's consider the following Cauchy's problem:

$$\begin{cases} \ddot{x}(t) = g(x(t), \dot{x}(t)) \\ x(0) = 2, \dot{x}(0) = 0, \end{cases} \quad (55)$$

where

$$g(x, y) := \begin{cases} -x & \text{if } x \geq 2 \\ 4(x-1) & \text{if } x < 2 \end{cases}$$

In this case g is discontinuous at the points of the form $(2, y), \forall y \in \mathbb{R}$.

Again we solve each part. Firstly we solve

$$\ddot{x}(t) = -x(t), \quad x(0) = 2, \quad \dot{x}(0) = 0, \quad (56)$$

whose solution is:

$$x(t) = 2\cos(t). \quad (57)$$

Secondly we solve

$$\ddot{x}(t) = 4(x(t) - 1), \quad x(0) = 2, \quad \dot{x}(0) = 0, \quad (58)$$

with solution

$$x(t) = \cosh(2t) + 1. \quad (59)$$

However, if we analyze each solution we realize that those solutions only holds for $t = 0$ and that there is no solution in any neighborhood of this point. Let's consider the Taylor series at 0 (initial condition point) for a hypothetical solution $x(t)$ (although $x(t)$ is not C^2 at $t = 0$, this condition is satisfied at both sides of it, so we can consider the Taylor series at a neighborhood of 0):

$$x(t) = x(0) + \dot{x}(0)t + \frac{\ddot{x}(\xi)}{2}t^2 = 2 + \frac{\ddot{x}(\xi)}{2}t^2, \quad (60)$$

for one ξ such that $0 < \xi < t$.

Hence, $\text{sign}(x(t) - 2) = \text{sign}(\ddot{x}(t))$. If $\text{sign}(x(t) - 2) > 0 \Rightarrow x(t) > 2$ but $\ddot{x}(t) = -x(t) < 0$ which is a contradiction. If $\text{sign}(x(t) - 2) < 0 \Rightarrow x(t) < 2$, however, $\ddot{x}(t) = 4(x(t) - 1)$ which is another contradiction if $x(t) > 1$ (the initial condition is $x(0) = 2$). Then there is no solution for problem (55).

The last example gives us a third option, a unique solution. Let's consider the following Cauchy problem:

$$\begin{cases} \ddot{x}(t) = g(x(t), \dot{x}(t)) \\ x(\frac{\pi}{4}) = 2\sqrt{2}, \quad \dot{x}(\frac{\pi}{4}) = 0. \end{cases} \quad (61)$$

At the initial conditions the function g is continuous and as $x(\frac{\pi}{4}) = 2\sqrt{2}$ we start solving the first branch whose solution is $x(t) = 2(\cos(t) + \sin(t))$. However, this time the solution leaves this branch at $t = \frac{\pi}{2}$. At that point the solution for the second branch is $e^{\pi-2t} + 1$. This solution does not leave the second branch for $t \geq \frac{\pi}{2}$, so there is a unique solution given by the following expression:

$$x(t) = \begin{cases} 2(\cos(t) + \sin(t)) & \text{if } \frac{\pi}{4} \leq t < \frac{\pi}{2} \\ e^{\pi-2t} + 1 & \text{if } t \geq \frac{\pi}{2} \end{cases} \quad (62)$$

Once observed that problems which are similar to ours could have no solution, one solution or several ones, it is necessary to study this question (existence and uniqueness) in detail.

As we have said previously the study of existence and uniqueness of solution in our system is not an easy task, indeed, it is a non-standard problem which can not be solved using the usual methods, so we are going to analyze it in the simple case of two pedestrians ($n = 2$). In this Appendix we will only consider the cases of normal force, only pushing force (exhaustive analysis on the plastic one) and normal force along with the plastic pushing force (the results with the other pushing forces are mainly the same).

Let's start studying the problem without pushing forces, this is $F^P \equiv 0$:

$$\begin{cases} m_1 \ddot{x}_1(t) = \kappa \tan\left(\frac{\pi}{2} \frac{\max(r-x_1(t), 0)}{r}\right) - \kappa \tan\left(\frac{\pi}{2} \frac{\max(x_1(t)-x_2(t)+2r, 0)}{2r}\right) \\ m_2 \ddot{x}_2(t) = \kappa \tan\left(\frac{\pi}{2} \frac{\max(x_1(t)-x_2(t)+2r, 0)}{2r}\right) - \kappa \tan\left(\frac{\pi}{2} \frac{\max(x_2(t)+r-L, 0)}{r}\right) \end{cases} \quad (63)$$

$$x_1(0) = x_{10}, \quad x_2(0) = x_{20}, \quad \dot{x}_1(0) = 0, \quad \dot{x}_2(0) = 0.$$

This one is a classical problem which can be solved through usual methods (considering the condition of the model $0 < x_{10} < x_{20} < L$). In this case we are going to show that the functions are continuous and locally Lipschitz continuous in its domain which ensures the existence of solution and at least the local uniqueness.

Firstly, we are going to study the continuity of normal forces. We consider $F^N(\Delta_1(t))$ (although the results could be generalized for any $\Delta_i(t)$).

$$F^N(\Delta_1(t)) = \kappa \cdot \tan\left(\frac{\pi}{2} \frac{\max(x_1(t) - x_2(t) + 2r, 0)}{2r}\right) \quad (64)$$

This function, F^N , is not continuous whenever the tangent is discontinuous, this is, whenever $\max(x_1(t) - x_2(t) + 2r, 0) = (2k - 1) \cdot 2r$, $k \in \mathbb{Z}$.

Then, if $0 \leq \frac{\max(x_1(t) - x_2(t) + 2r, 0)}{2r} < 1$, $F^N(\Delta_1(t))$ is continuous. If $x_1(t) - x_2(t) + 2r \leq$

0 then $F^N(\Delta_1(t)) \equiv 0$, which is obviously continuous. On the other hand, if $x_1(t) - x_2(t) + 2r > 0$, $F^N(\Delta_1(t))$ is continuous whenever $\frac{\max(x_1(t) - x_2(t) + 2r, 0)}{2r} < 1$. By the condition given by the model $x_{10} < x_{20}$, so $x_1(t) < x_2(t), \forall t \in [0, h]$ for one $h > 0$. Then $\frac{\max(x_1(t) - x_2(t) + 2r, 0)}{2r} = 1 + \frac{x_1(t) - x_2(t)}{2r} < 1, \forall t \in [0, h]$ and consequently $F^N(\Delta_1(t))$ is continuous at least in a neighborhood of 0.

Now, we want to prove the local uniqueness, so we are going to show that $F^N(\Delta_1(t))$ is locally Lipschitz. Firstly, we can easily check that $\max(x, 0)$ is globally Lipschitz continuous with Lipschitz constant 1. Meanwhile tangent function is continuous differentiable in $(-\frac{\pi}{2}, \frac{\pi}{2})$, so $\tan(\frac{\pi}{2}x)$ is continuous differentiable in $(-1, 1)$ and consequently is locally Lipschitz in that interval. Finally, as the composition of continuous Lipschitz functions is again a continuous Lipschitz function we can ensure that at least there is a local unique solution.

The second case we are going to study is just considering the plastic pushing force (without normal force, this is, $F^N \equiv 0$). Then, the problem we are going to analyze is:

$$\begin{cases} m_1 \ddot{x}_1(t) = -F^P(\Delta_1(t), \dot{\Delta}_1(t)) \\ m_2 \ddot{x}_2(t) = F^P(\Delta_1(t), \dot{\Delta}_1(t)) \end{cases} \quad (65)$$

$$x_1(0) = x_{10}, \quad x_2(0) = x_{20}, \quad \dot{x}_1(0) = 0, \quad \dot{x}_2(0) = 0.$$

Let's analyze each pushing force (F^{HR} , F^A and F^{Pl}).

Firstly we are going to analyze the case $F^P = F^{HR}$. Let's remember the form of this function defined in section 4

$$F^{HR}(\Delta_1(t), \dot{\Delta}_1(t)) := \begin{cases} \frac{P}{2}(\frac{2}{\pi} \arctan(\beta\Delta_1(t)) + 1) & \text{if } \dot{\Delta}_1(t) > 0 \\ \frac{P}{2}(\frac{2}{\pi} \arctan(\beta(\Delta_1(t) - \Delta_0)) + 1) & \text{if } \dot{\Delta}_1(t) \leq 0 \end{cases} \quad (66)$$

Arctangent function is continuous in \mathbb{R} and globally Lipschitz continuous so the discontinuity problem of this force resides in the points whenever $\dot{\Delta}_1(t) = 0$, this is, whenever $\dot{x}_1(t) = \dot{x}_2(t)$. As two of the initial conditions are $\dot{x}_1(0) = 0$ and $\dot{x}_2(0) = 0$, then if this force is considered in our system we cannot use classical analysis at least at the beginning.

Secondly, we will study the scenario in which $F^P = F^A$. Again, we consider the form of this function in section 4:

$$F^A(\Delta_1(t), \dot{\Delta}_1(t)) = \begin{cases} m\Delta_1(t) & \text{if } 0 \leq \dot{\Delta}_1(t) \wedge \Delta_1(t) > 0 \\ M(\Delta_1(t) - d_0) & \text{if } 0 > \dot{\Delta}_1(t) \wedge \Delta_1(t) > 0 \\ 0 & \text{otherwise} \end{cases} \quad (67)$$

As in the previous case, each branch of F^A is continuous and Lipschitz continuous (all of them are linear functions) so the existence and uniqueness problem is found in the points in which the branches join discontinuously, this is, whenever $\Delta_1(t) > 0, \dot{\Delta}_1(t) = 0$ or $\Delta_1(t) = 0, \dot{\Delta}_1(t) < 0$. As two of the initial conditions are

$\dot{x}_1(0) = 0$ and $\dot{x}_2(0) = 0$, if x_{10}, x_{20} are such that $\Delta_1(0) \leq 0$ then we are not in a discontinuity point and there is a local unique solution, however, if x_{10}, x_{20} are such that $\Delta_1(0) > 0$ then our initial conditions are given in a discontinuous point and then a non classical analysis must be carried out.

Finally, we are going to analyze the case $F^P = F^{Pl}$. Remembering the definition of F^{Pl} in section 4:

$$F^{Pl}(\Delta_1(t), \dot{\Delta}_1(t)) = \begin{cases} m_p \Delta_1(t) & \text{if } \dot{\Delta}_1(t) > 0 \wedge \Delta_1(t) > 0 \\ M_p(\Delta_1(t) - d_p) & \text{if } \dot{\Delta}_1(t) \leq 0 \wedge \Delta_1(t) > d_p \\ 0 & \text{otherwise} \end{cases} \quad (68)$$

Like it happened previously, each branch of F^{Pl} is continuous and Lipschitz continuous so the existence and local uniqueness is ensured at every point except those in which the branches link discontinuously, namely, whenever $\dot{\Delta}_1(t) = 0, \Delta_1(t) > 0, \Delta_1(t) \neq d_p, \Delta_1(t) \neq 2r$. Again two of the initial conditions are $\dot{x}_1(0) = 0$ and $\dot{x}_2(0) = 0$, so if x_{10}, x_{20} are such that $\Delta_1(0) < 0$ then we are not in a discontinuity point and there is a local unique solution; however, if x_{10}, x_{20} are such that $\Delta_1(0) > 0, \Delta_1(0) \neq d_p, x_{10} < x_{20}$, then the initial conditions are given in a discontinuous point and then we must analyze the existence and uniqueness by using non-classical results.

Coming back to the problem (65), let us consider $F^P = F^{Pl}$ and $m_1 = m_2 = 1$ in order to simplify the problem. Then we easily verify that $\ddot{x}_1(t) + \ddot{x}_2(t) = 0$. This implies that under the given conditions $\dot{x}_1(t) + \dot{x}_2(t) = 0$ and $x_1(t) + x_2(t) = c_1$ where $c_1 = x_1(0) + x_2(0) = x_{10} + x_{20}$. Isolating $x_2(t)$ we obtain:

$$x_2(t) = x_{10} + x_{20} - x_1(t) \quad (69)$$

Substituting in (65) and renaming $\alpha = x_{10} + x_{20} - 2r$ and $\gamma = \alpha + d_p$ (as $d_p > 0, \gamma > \alpha$) we reduce our system to:

$$\ddot{x}_1(t) = \begin{cases} -m_p(2x_1(t) - \alpha) & \text{if } \dot{x}_1(t) > 0 \wedge 2x_1(t) > \alpha \\ -M_p(2x_1(t) - \gamma) & \text{if } \dot{x}_1(t) \leq 0 \wedge 2x_1(t) > \gamma \\ 0 & \text{otherwise} \end{cases} \quad (70)$$

$$x_1(0) = x_{10}, \quad \dot{x}_1(0) = 0.$$

Following the same procedure as for (47) and (55), we split it into the following three Cauchy problems:

$$\ddot{x}_1(t) = -m_p(2x_1(t) - \alpha), \quad x_1(0) = x_{10}, \quad \dot{x}_1(0) = 0. \quad (71)$$

$$\ddot{x}_1(t) = -M_p(2x_1(t) - \gamma), \quad x_1(0) = x_{10}, \quad \dot{x}_1(0) = 0. \quad (72)$$

$$\ddot{x}_1(t) = 0, \quad x_1(0) = x_{10}, \quad \dot{x}_1(0) = 0, \quad (73)$$

whose solutions are, respectively,

$$x_1(t) = (x_{10} - \frac{\alpha}{2})\cos(\sqrt{2m_p}t) + \frac{\alpha}{2}, \quad (74)$$

$$x_1(t) = (x_{10} - \frac{\gamma}{2})\cos(\sqrt{2M_p}t) + \frac{\gamma}{2}, \quad (75)$$

and

$$x_1(t) \equiv x_{10}. \quad (76)$$

If we consider $\Delta_1(0) = x_{10} - x_{20} + 2r < 0$ ($\Leftrightarrow 2x_{10} < \alpha$), then clearly the unique solution is $x_1(t) \equiv x_{10}$, $x_2(t) \equiv x_{20}$.

Let's study the more interesting case when $\Delta_1(0) > 0$. If $2x_{10} \in (\alpha, \gamma)$ the solution is still $x_1(t) \equiv x_{10}$, $x_2(t) \equiv x_{10}$, $\forall t, t > 0$. If $\Delta_1(0) > d_p$, this is, $2x_{10} > \gamma$ the unique solution is $x_1(t) = (x_{10} - \frac{\gamma}{2})\cos(\sqrt{2M_p}t) + \frac{\gamma}{2}$, $x_2(t) = x_{10} + x_{20} - (x_{10} - \frac{\gamma}{2})\cos(\sqrt{2M_p}t) + \frac{\gamma}{2}$, $\forall t \in [0, h]$ for some $h > 0$. Then, as $2x_{10} > \gamma$, and $\dot{x}_1(t) = -((x_{10} - \frac{\gamma}{2})\sqrt{2M_p}\sin(\sqrt{2M_p}t)) < 0$, $\forall t \in [0, h]$ such that $x_1(t) > \frac{\gamma}{2}$, there is a unique local solution at least in a neighborhood of 0.

Finally we are going to study the case including normal forces and plastic pushing forces. The system of equations is given by the following expression:

$$\begin{cases} \ddot{x}_1(t) = F^{NL}(t) - F^N(\Delta_1(t)) - F^{Pl}(\Delta_1(t), \dot{\Delta}_1(t)) \\ \ddot{x}_2(t) = -F^{NR}(t) + F^N(\Delta_1(t)) + F^{Pl}(\Delta_1(t), \dot{\Delta}_1(t)) \end{cases} \quad (77)$$

$$x_1(0) = x_{10}, \quad x_2(0) = x_{20}, \quad \dot{x}_1(0) = 0, \quad \dot{x}_2(0) = 0.$$

As it is still difficult to be studied directly in this form, we are going to divide it into several scenarios.

Considering $L = 2nr = 4r$, the first scenario is whenever $x_1(0) = x_{10} = r$, $x_2(0) = x_{20} = 3r$. In this case initially all the forces are equal to 0 and then the unique solution is $x_1(t) \equiv x_{10} = r$, $x_2(t) \equiv x_{20} = 3r$, $\forall t > 0$.

The second one is whenever $r < x_1(0) = x_{10} < x_2(0) = x_{20} < L - r = 3r$. In this case, initially the system can be simplified obtaining:

$$\begin{cases} \ddot{x}_1(t) = -F^N(\Delta_1(t)) - F^{Pl}(\Delta_1(t), \dot{\Delta}_1(t)) \\ \ddot{x}_2(t) = F^N(\Delta_1(t)) + F^{Pl}(\Delta_1(t), \dot{\Delta}_1(t)) \end{cases} \quad (78)$$

$$x_1(0) = x_{10}, \quad x_2(0) = x_{20}, \quad \dot{x}_1(0) = 0, \quad \dot{x}_2(0) = 0.$$

Then, the following relation still holds in a neighborhood of 0:

$$\ddot{x}_1(t) + \ddot{x}_2(t) \equiv 0, \quad (79)$$

and by the initial conditions

$$\dot{x}_1(t) + \dot{x}_2(t) \equiv 0, \quad (80)$$

$$x_1(t) + x_2(t) \equiv x_{10} + x_{20}. \quad (81)$$

As previously, $x_2(t) = x_{10} + x_{20} - x_1(t)$. Substituting it in the system of equations we obtain a single equation:

$$\begin{aligned} \ddot{x}_1(t) = & -\kappa \tan\left(\frac{\pi}{2} \frac{\max(2x_1(t) - \alpha, 0)}{2r}\right) - \\ & - \begin{cases} m_p(2x_1(t) - \alpha) & \text{if } \dot{x}_1(t) > 0 \wedge 2x_1(t) > \alpha \\ M_p(2x_1(t) - \gamma) & \text{if } \dot{x}_1(t) \leq 0 \wedge 2x_1(t) > \gamma \\ 0 & \text{otherwise} \end{cases} \end{aligned} \quad (82)$$

Following the previous process we split it into three problems:

$$\ddot{x}_1(t) = -\kappa \tan\left(\frac{\pi}{2} \frac{\max(2x_1(t) - \alpha, 0)}{2r}\right) - m_p(2x_1(t) - \alpha), \quad x_1(0) = x_{10}, \quad \dot{x}_1(0) = 0. \quad (83)$$

$$\ddot{x}_1(t) = -\kappa \tan\left(\frac{\pi}{2} \frac{\max(2x_1(t) - \alpha, 0)}{2r}\right) - M_p(2x_1(t) - \gamma), \quad x_1(0) = x_{10}, \quad \dot{x}_1(0) = 0. \quad (84)$$

$$\ddot{x}_1(t) = -\kappa \tan\left(\frac{\pi}{2} \frac{\max(2x_1(t) - \alpha, 0)}{2r}\right), \quad x_1(0) = x_{10}, \quad \dot{x}_1(0) = 0. \quad (85)$$

If $2x_{10} < \alpha$ then initially $\ddot{x}_1(t) = 0$, so $x_1(t) \equiv x_{10}, x_2(t) \equiv x_{20}, \forall t \geq 0$. If $2x_{10} > \gamma$ then $\ddot{x}_1(0) < 0$ so the first derivative is monotonically decreasing. As $\dot{x}_1(0) = 0$ then for any $t > 0, \dot{x}_1(t) < 0$. In this case we are in the branch (84) where the functions are continuous with continuous derivative and consequently there is a unique solution at least locally.

The case $\alpha < 2x_{10} < \gamma$ remains open for us.

The third scenario is whenever $0 < x_{10} < r < L - r = 3r < x_{20} < L$. It implies that $2x_{10} < \alpha$. Then, initially we obtain the following system of equations:

$$\begin{cases} \ddot{x}_1(t) = F^{NL}(t) \\ \ddot{x}_2(t) = -F^{NR}(t) \end{cases} \quad (86)$$

$$x_1(0) = x_{10}, \quad x_2(0) = x_{20}, \quad \dot{x}_1(0) = 0, \quad \dot{x}_2(0) = 0.$$

Similarly to what happened in (63) this is a classical problem and there is a unique solution at least locally.

The last case to study is whenever $0 < x_{10} < r$ and $x_{20} < L - r = 3r$ (which is analogous to the case in where $x_{20} > L - r$ and $x_{10} > r$). Then, initially the system is reduced to

$$\begin{cases} \ddot{x}_1(t) = F^{NL}(t) - F^N(\Delta_1(t)) - F^{Pl}(\Delta_1(t), \dot{\Delta}_1(t)) \\ \ddot{x}_2(t) = F^N(\Delta_1(t)) + F^{Pl}(\Delta_1(t), \dot{\Delta}_1(t)) \end{cases} \quad (87)$$

$$x_1(0) = x_{10}, \quad x_2(0) = x_{20}, \quad \dot{x}_1(0) = 0, \quad \dot{x}_2(0) = 0.$$

We discuss three different scenarios. The first one is the case $\Delta_1(0) < 0$ (this implies $F^N(\Delta_1(0)) = 0$ and $F^{Pl}(\Delta_1(0), \dot{\Delta}_1(0)) = 0$) and the remaining problem is at least at the beginning

$$\begin{cases} \ddot{x}_1(t) = \kappa \tan\left(\frac{\pi}{2r} \max(r - x_1(t), 0)\right) \\ \ddot{x}_2(t) = 0 \end{cases} \quad (88)$$

$$x_1(0) = x_{10}, \quad x_2(0) = x_{20}, \quad \dot{x}_1(0) = 0, \quad \dot{x}_2(0) = 0,$$

and, as in previous cases, there is a locally unique solution with $x_2(t) \equiv x_{20}$.

The second one is whenever $\Delta_1(0) > d_p$, this is, $2x_{10} > \gamma$. In this situation we remember that initially problem under study is the following

$$\begin{cases} \ddot{x}_1(t) = \kappa \tan\left(\frac{\pi}{2r} \max(r - x_1(t), 0)\right) - \kappa \tan\left(\frac{\pi}{4r} \max(x_1(t) - x_2(t) + 2r, 0)\right) - \\ \quad - \begin{cases} m_p \Delta_1(t) & \text{if } \dot{\Delta}_1(t) > 0 \wedge \Delta_1(t) > 0 \\ M_p(\Delta_1(t) - d_p) & \text{if } \dot{\Delta}_1(t) \leq 0 \wedge \Delta_1(t) > d_p \\ 0 & \text{otherwise} \end{cases} \\ \ddot{x}_2(t) = +\kappa \tan\left(\frac{\pi}{4r} \max(x_1(t) - x_2(t) + 2r, 0)\right) + \\ \quad + \begin{cases} m_p \Delta_1(t) & \text{if } \dot{\Delta}_1(t) > 0 \wedge \Delta_1(t) > 0 \\ M_p(\Delta_1(t) - d_p) & \text{if } \dot{\Delta}_1(t) \leq 0 \wedge \Delta_1(t) > d_p \\ 0 & \text{otherwise} \end{cases} \end{cases} \quad (89)$$

$$x_1(0) = x_{10}, \quad x_2(0) = x_{20}, \quad \dot{x}_1(0) = 0, \quad \dot{x}_2(0) = 0.$$

As a consequence of $\Delta_1(0) > d_p$, when $3x_{10} > x_{20}$, $\max(x_1(t) - x_2(t) + 2r, 0) > 2\max(r - x_1(t), 0)$, $\forall t \in [0, h]$ for some $h > 0$. It implies that $\ddot{x}_1(t) < 0$, $\forall t \in [0, h]$ for some $h > 0$. Moreover, $\dot{x}_2(t) > 0$, $\forall t \geq 0$ and then $\dot{\Delta}_1(t) < 0$, $\forall t \in [0, h]$ and we are not going to leave the second branch. By this fact, at least locally, there will not be any discontinuity and then there is a local unique solution.

We have not found yet any proof for the third case, this is, whenever $0 \leq \Delta_1(0) \leq d_p$.

In conclusion, we have proved that there is at least a local unique solution in most of the cases under certain conditions in order to simplify the problem.

13 Appendixes references

- [8] J. R. Dormand, P.J. Prince, "A family of embedded Runge-Kutta formulae", *Journal of Computational and Applied Mathematics* **6(1)**: 19–26 (1980)
- [9] T. Kimura, *On Dormand-Prince method* (2009). Retrieved May 02, 2016 from http://depa.fquim.unam.mx/amyd/archivero/DormandPrince_19856.pdf